Accepted manuscript
Bura-Nakić, E., Andersen, M. B., Archer, C., de Souza, G. F., Marguš, M., & Vance, D. (2018). Coupled Mo-U abundances and isotopes in a small marine euxinic basin: Constraints on processes in euxinic basins. *Geochimica et Cosmochimica Acta*, *222*, 212–229. https://doi.org/10.1016/j.gca.2017.10.023

Coupled Mo-U abundances and isotopes in a small marine euxinic basin: constraints on processes in euxinic basins

Elvira Bura-Nakic[1,2], Morten, B. Andersen[1,3*], Corey Archer[1], Gregory F. de Souza[1], Marija Marguš[2], Derek Vance[1]

[1] Institute of Geochemistry and Petrology, Department of Earth Sciences, ETH Zürich, Clausiusstrasse 25, 8092 Zürich, Switzerland.

[2] Division for Marine and Environmental Research, Ruđer Bošković Institute, Bijenička 54, HR-10002, Zagreb, Croatia.

[3] School of Earth and Ocean Sciences, Cardiff University, Cardiff, UK.

* Corresponding author (andersenm1@cardiff.ac.uk)

~9500 words in main text

8 figures

1 table

5 supplementary tables and one supplementary text

Abstract

Sedimentary molybdenum (Mo) and uranium (U) abundances, as well as their isotope systematics, are used to reconstruct the evolution of the oxygenation state of the surface Earth from the geological record. Their utility in this endeavour must be underpinned by a thorough understanding of their behaviour in modern settings. In this study, Mo-U concentrations and their isotope compositions were measured in the water column, sinking particles, sediments and pore waters of the marine euxinic Lake Rogoznica (Adriatic Sea, Croatia) over a two year period, with the aim of shedding light on the specific processes that control Mo-U accumulation and isotope fractionations in anoxic sediment.

Lake Rogoznica is a 15 m deep stratified sea-lake that is anoxic and euxinic at depth. The deep euxinic part of the lake generally shows Mo depletions consistent with near-quantitative Mo removal and uptake into sediments, with Mo isotope compositions close to the oceanic composition. The data also, however, show evidence for periodic additions of isotopically light Mo to the lake waters, possibly released from authigenic precipitates formed in the upper oxic layer and subsequently processed through the euxinic layer. The data also show evidence for a small isotopic offset (~0.3‰ on $^{98}Mo/^{95}Mo$) between particulate and dissolved Mo, even at highest sulfide concentrations, suggesting minor Mo isotope fractionation during uptake into euxinic sediments. Uranium concentrations decrease towards the bottom of the lake, where it also becomes isotopically lighter. The U systematics in the lake show clear evidence for a dominant U removal mechanism via diffusion into, and precipitation in, euxinic sediments, though the diffusion profile is mixed away under conditions of increased density stratification between an upper oxic and lower anoxic layer. The U diffusion-driven precipitation is best described with an effective $^{238}U/^{235}U$ fractionation of +0.6‰, in line with other studied euxinic basins.

Combining the Mo and U systematics in Lake Rogoznica and other euxinic basins, it is apparent that the two different uptake mechanisms of U and Mo can lead to spatially and temporally variable Mo/U and Mo-U isotope systematics that depend on the rate of water renewal versus removal to sediment, the sulfide concentration, and the geometry of the basin. This study further emphasises the potential of combining multiple observations, from Mo-U enrichment and isotope systematics, for disentangling the various processes via which redox conditions control the chemistry of modern and ancient sediments.

1. Introduction

The sedimentary abundances and isotopic compositions of redox sensitive trace metals play a prominent role in attempts to reconstruct the history of surface Earth oxygenation. Of all the redox sensitive metals that have been used, molybdenum (Mo) and uranium (U) have perhaps been the most prominent. Both are soluble under oxidizing conditions and exhibit conservative behaviour in the open ocean, with residence times that are significantly longer than ocean mixing times (800 and 250–500 kyr respectively, Emerson and Huested, 1991). In some anoxic or euxinic (i.e. anoxic and sulfidic) settings, on the other hand, both Mo and U show non-conservative behaviour in the water column and are variably removed to sediment, though probably via different extraction mechanisms (Ku et al., 1977; Collier, 1985; McLennan, 2001; Algeo and Tribovillard, 2009; Nakagawa et al., 2012; Tribovillard et al., 2012). Organic-rich, reducing sediments are the most important modern oceanic Mo and U sinks (Emerson and Huested, 1991; Morford and Emerson, 1999; McManus et al., 2006; Scott et al., 2008). Coupled analysis of Mo and U authigenic enrichment in reducing organic-rich sediments has been used to investigate the degree of anoxia prevailing in the past water column (e.g., Scott et al., 2008; Algeo and Tribovillard, 2009; Tribovillard et al., 2012).

The Mo and parent U isotopic composition of ancient black shales are also thought to be related to the redox state of the global ocean, as Mo and U isotopes are fractionated differently in oxic and anoxic ocean sinks (e.g. Barling et al., 2001; Siebert et al., 2003; Arnold et al., 2004; Stirling et al., 2007; Weyer et al., 2008; Gordon et al., 2009; Montoya-Pino et al., 2010; Scheiderich et al., 2010; Voegelin et al., 2010; Brennecka et al., 2011a; Herrmann et al., 2012; Azrieli-Tal et al., 2014; Dahl et al., 2014; Westermann et al., 2014). The conservative behaviour of Mo in oxygenated waters arises from the fact that the main Mo species, molybdate ($Mo^{VI}O_4^{2-}$), has a low particle affinity, leading to the relatively long residence time of Mo in the oceans (Emerson and Huested, 1991). In such oxidizing environments, slow adsorption of dissolved Mo to Mn

oxide particles preferentially accumulates light Mo isotopes in the particulate phase (by ~ 3‰ for $^{98}Mo/^{95}Mo$; Barling and Anbar, 2004), leaving the dissolved Mo pool enriched in heavy Mo isotopes (Barling and Anbar, 2004). In contrast, under euxinic conditions, with significant dissolved sulfide, oxygen atoms in molybdate can be replaced with sulfur atoms (Erickson and Helz, 2000; Vorlicek and Helz, 2002). The product thiomolybdate ($Mo^{VI}O_nS_4^{2-}$) species are particle reactive, readily scavenged (e.g. by particulate Fe and organic matter), and thus removed from the water column into the underlying sediments (Helz et al., 1996; Vorlicek and Helz, 2002; Bostick et al., 2003). At sulfide concentrations greater than ~11 µmol l^{-1} the conversion of molybdate to tetrathiomolybdate ($Mo^{VI}S_4^{2-}$) is nearly complete (Erickson and Helz, 2000). Thus, in highly restricted anoxic basins, such as the Black Sea ($[\Sigma S^{-II}]$ ~300 µmol l^{-1}, Emerson and Huested 1991) the conversion of $Mo^{VI}O_4^{2-}$ to $Mo^{VI}S_4^{2-}$ is almost complete at depth, leading to near-quantitative molybdenum removal from the water column. Accordingly, in the underlying sediment, authigenic Mo records a Mo isotopic composition that is very close to the original seawater composition (Nägler et al., 2011). The process of conversion to sulfidic species does, however, involve Mo isotope fractionation (Tossell, 2005; Kerl et al., 2017), which may be expressed in mildly euxinic conditions when intermediate products in the $Mo^{VI}O_4^{2-}$ to $Mo^{VI}S_4^{2-}$ conversion are present and when conversion to tetrathiomolybdate is not complete. Furthermore, there appears to be a small isotopic difference between aqueous $Mo^{VI}S_4^{2-}$ and authigenic solid Mo, with $\Delta^{98/95}Mo_{tetrathiomo\text{-}sediment} = +0.5 \pm 0.3$‰ (Nägler et al., 2011).

Uranium, in the form of U^{6+}, mainly forms highly soluble complexes with carbonate species in oxic seawater, again leading to the relatively long residence time (Morford and Emerson, 1999). In contrast, the reduced U^{4+} species is highly insoluble. Large variations in the ratio of uranium's long-lived isotopes $^{238}U/^{235}U$ have been observed under redox-controlled U^{6+}-U^{4+} exchange in low-temperature environments (Stirling et al., 2007; Weyer et al., 2008). Oxic

adsorption of U to ferromanganese oxides without redox change, and under oxic conditions, results in a small fractionation of the $^{238}U/^{235}U$ ratio ($\delta^{238/235}U_{soln\text{-}MnOx}$ = ~0.2‰; Brennecka et al., 2011b). On the other hand, the incorporation of U^{4+} into anoxic sediments generally leads to significant (permil level) enrichment of the heavier isotope, ^{238}U, in sediment (e.g. Weyer et al., 2008; Andersen et al., 2014). In contrast to Mo, typical processes for U removal into anoxic sediments have been suggested to involve U transported with sinking particulate organic matter (Anderson et al. 1989b; Zheng et al., 2002) and diffusion of seawater U into sediment pore waters and reduction within the sediment itself (Anderson et al., 1989a; Barnes and Cochran, 1990; Klinkhammer and Palmer, 1991). Although still a matter of some debate, the latter process has been determined to dominate the authigenic U flux in most studied anoxic marine settings (e.g. Anderson 1987; McManus et al 2005). Furthermore, the mechanistic nature of U fixation within anoxic sediment is also still debated, but likely dominated by metal- and sulfate-reducing bacteria that use U^{VI} as an electron acceptor (Lovley et al., 1991; Bargar et al., 2013).

As a result, while the Mo isotopic composition of seawater may be directly recorded in sediments accumulated under strongly euxinic conditions via near-quantitative Mo uptake, U is taken up less quantitatively and U isotopes generally display large fractionations between anoxic organic-rich sediments and seawater (Weyer et al., 2008; Andersen et al., 2014; Noordmann et al., 2015; Holmden et al., 2015; Andersen et al., 2016; Rolison et al., 2017). As Mo and U display significant isotope fractionations between oxic and anoxic sinks, both isotope systems have the potential to record the redox evolution of the global ocean. However, the investigation of Mo and U behaviour in different modern settings has revealed significant Mo isotope fractionation in sediments deposited under suboxic as well as under anoxic water columns bearing low sulfide concentrations (Siebert et al., 2003; Siebert et al., 2006; Poulson et al., 2006; Poulson Brucker et al., 2009; Nägler et al., 2011). In addition to Mo removal in

euxinic waters, other processes have been invoked to control sedimentary Mo isotopes in anoxic settings. These include the delivery of Mo with light Mo isotope compositions to euxinic sediments or bottom water on Fe-Mn oxyhydroxide-rich particulates (e.g. Barling and Anbar, 2004; Goldberg et al., 2009), adsorption of Mo to organic matter with an isotopic fractionation (Kowalski et al., 2013) and early diagenetic redistribution of Mo within sediment and pore-waters (McManus et al., 2002). Studies reporting the U isotopic composition of anoxic to suboxic sediments have shown not only a significant U isotopic fractionation in comparison to seawater, but also variable fractionation between these modern anoxic settings. While several studies suggest an apparent U isotope fractionation factor (ε) for $^{238}U/^{235}U$ in the range of ~+0.5 to 0.8‰ during U uptake in anoxic sediments (Weyer et al. 2008; Andersen et al., 2014; Holmden et al., 2015; Noordmann et al., 2015; Andersen et al., 2016, Rolison et al., 2017) both significantly higher and lower U isotope compositions have been observed in anoxic sediments (Weyer et al. 2008; Montoya-Pino et al. 2010; Noordmann et al., 2015; Hinojosa et al. 2016). This suggests further mechanisms for U withdrawal from the anoxic water columns, or variable U isotope mass-balance during non-quantitative authigenic U sediment uptake (Andersen et al., 2017).

To improve our understanding of the behaviour of Mo and U and their isotopes, further studies in well-characterised modern settings are needed. In this study, Mo and U concentrations and isotope compositions of the water column, sinking particles, sediments and pore waters of the marine euxinic Lake Rogoznica, Croatia, are presented. Based on the comprehensive dataset obtained, including seasonal patterns, we shed further light on the processes controlling Mo and U isotope fractionation mechanisms in anoxic water columns and their sediments.

2. Methods

2.1. Study site

Lake Rogoznica is a small, intensely eutrophicated sea-lake situated on the eastern coast of the Adriatic Sea (Ciglenečki et al., 2005; Bura-Nakić et al., 2009; Ciglenečki et al., 2015). The lake is surrounded by sheer carbonate cliffs (4–23 m above mean sea-level), has a surface area of about 5300 m^2 and a maximum depth of ~15 m. Due to its stratification, and despite permanent water exchange with the surrounding sea through porous karst, Lake Rogoznica becomes anoxic at depth due to the remineralisation of organic matter produced in periods of intense primary production (blooms) near the surface (Ciglenečki et al., 2005; Bura-Nakić et al., 2009; Ciglenečki et al., 2015). It is therefore well-suited for studying biogeochemical processes influencing redox-sensitive trace metals. Complete vertical mixing of the lake, where cold oxygen-rich water from the surface mixes downwards and anoxic deep waters are brought to the surface, often occurs during the dry and cold autumn period. Complete mixing of the lake, leading to catastrophic anoxia in the whole water column, occurs rarely, once or twice in every 10 winters depending on the meteorological conditions (Ciglenečki et al., 2005; 2015). Under stratified conditions, the surface water is well oxygenated while the layer below approx. 9 m depth is anoxic. The anoxic deep waters become rich in sulfur (up to 5000 μmol l^{-1}) predominantly in the form of sulfide (Ciglenečki et al., 2005; Bura-Nakić et al., 2009; Ciglenečki et al., 2015).

2.2. Sampling and sample collection

Prior to field work, syringes, bottles, tygon tubes and all other materials used for sediment and water column sampling were pre-cleaned in ~3 N HCl and rinsed with MQ water (18 MΩ·cm). Unless otherwise stated, all reagents used were sub-boiling distilled twice in teflon stills.

Water column samples were collected from the middle of the lake during six campaigns spanning 2013 (February, April, July and October) and 2015 (April and July). All water samples

were collected by lowering a custom-made (30 cm diameter) filter housing down into the lake, so that filtration occurred *in situ*, and the water was pumped through a 0.2 µm mesh-sized filter (Millipore, Whatman 47 mm diameter PTFE) to the surface using silicone tubing (0.9 cm outer diameter) and a Pegasus peristaltic pump. Approximately one litre was collected at each depth. All filtered samples were collected in pre-cleaned HDPE bottles and acidified (*p*H 2, using concentrated HCl). Salinity and oxygen concentration were measured *in situ* during the sampling using a HQ40D multimeter probe (HachLange, Germany). Sulfide concentrations were analysed by linear sweep voltammetry (LSV) within 8 hours of sampling according to procedures described elsewhere (Ciglenečki et al., 2005; Bura-Nakić et al., 2009; Ciglenečki et al., 2015). Electrochemical measurements were performed with µAutolab Electrochemical Instruments (EcoChemie) connected with 663VA Stand Metrohm electrode. *In situ* measurements of *p*H were performed during three sampling campaigns (October 2013, April and July 2015) using a HQ40D multimeter probe (HachLange, Germany). The *p*H values measured *in situ* were used to calculate $[H_2S]_{aq}$ following Millero et al. (1986, Supplementary Table 2).

One sediment core (~60 cm long) was collected in July 2013 from the middle and deepest part of Lake Rogoznica (~15 m) using an Uwitec gravity corer. Immediately after sampling, the core was sectioned into 5 cm segments in a glove box under N_2 overpressure. Pore water was extracted by centrifugation at 4000 rpm for 30 minutes. The pore water samples (10 to 30 ml) were transferred into HPDE bottles and acidified (*p*H 2) using concentrated HCl. A sample of the carbonate rock surrounding the lake was collected in April 2015, stored in a plastic bag, and cut into smaller pieces (1–2 g) using a diamond-blade saw.

2.3. Sample preparation

Chemical preparation and analysis of the samples were performed in the isotope facilities at the Institute of Geochemistry and Petrology, Department of Earth Sciences, ETH Zürich, Switzerland. Lake Rogoznica water column dissolved and particulates, as well as pore water and sediment samples were measured for selected elemental concentrations, and Mo and U isotopes. Elemental concentrations were measured in all samples (section 2.5) prior to preparation for isotope composition determination.

Water sample aliquots (varying from 20 to 150 ml) were taken for isotopic analysis, aiming for a total of 20–50 ng U and 150–250 ng Mo. These were transferred into pre-cleaned Teflon jars for the isotope determination, and spiked with the IRMM–3636 ^{236}U–^{233}U double-spike (Richter et al., 2008) aiming for a $^{236}U/^{235}U$ of ~4, and a ^{100}Mo–^{97}Mo double-spike (Archer and Vance, 2008) aiming for a 1:1 spike to sample ratio. These water sample aliquots were subsequently dried down (all at 100 °C). Due to the high Na–content, a large NaCl precipitate would form during this step. To obtain a more pure metal fraction, samples were leached using 10 ml 7 N HCl for 24 hours, a treatment which dissolves Mo, U and other metals but minimises dissolution of NaCl. The samples were then centrifuged (3500 rpm for 10 minutes), and the supernatant taken for analysis. The recoveries of both U and Mo in the supernatant were consistently >90% using this procedure. The supernatant was then dried down and re-dissolved in 5 ml 7 N HCl in preparation for column chromatography.

Filters used for the water filtration were dissolved in 10 ml of concentrated HNO_3 in pre-cleaned 60 ml Teflon beakers and dried down (all at 100 °C). Samples were then re-dissolved and fluxed in a 2 ml mixture of conc. HNO_3 and H_2O_2 (Merck Superpure, 1:1 ratio) on a hotplate for 24 hours, before being dried down. They were then re-dissolved in 5 ml of 7 N HCl and an aliquot (100 µL) was taken to determine elemental concentrations. The filters held 28 to 148 ng Mo and 3 to 23 ng U, while the total blanks for dissolution of clean unused filters in the same manner were ~40 pg for Mo and <1 pg for U (Supplementary Table 1). The samples were spiked

with the U and Mo double-spikes as described above, and left in closed Teflon beakers to equilibrate on a hotplate (100 °C) before column chromatography.

The pore water samples were weighed, dried down in pre-cleaned Teflon beakers, and pre-treated with the mixture of concentrated HNO_3 and H_2O_2 in a 1:1 ratio on a hotplate for 24 hours. Samples were then re-dissolved in 5 ml 7 N HCl and an aliquot taken to determine the elemental concentrations. Samples containing 70–170 ng Mo and 4–35 ng U were then spiked with the U and Mo double-spikes and left to equilibrate on a hotplate in preparation for column chromatography.

Approximately 50–100 mg of the sediment samples was used for analysis. Full dissolution of sediments was carried out using conventional protocols for silicates, involving mixtures of HF–HNO_3–HCl and H_2O_2 in the same manner described in Andersen et al. (2013). After final dissolution in 10 ml 6 N HCl, an aliquot was taken to determine elemental concentrations. An aliquot containing 20–50 ng U and 150–250 ng Mo was added to pre-cleaned Teflon beakers, spiked with the U and Mo double-spikes, and then left to equilibrate on a hotplate before being dried down (all at 100 °C). Samples were then re-dissolved in 5 ml 7 N HCl in preparation for column chromatography.

The carbonate rock sample was weighed and dissolved in a pre-cleaned Teflon beaker. The initial carbonate rock dissolution was performed in a 5 ml mixture of conc. HCl and H_2O in a 1:1 ratio for 24 hours. The sample was then dried down and pre-treated on a hotplate for 24 hours with a mixture of conc. HNO_3 and H_2O_2 in a 1:1 ratio. After final dissolution in 10 ml of 0.3 N HNO_3 an aliquot was taken to determine elemental concentrations. An aliquot containing ~50 ng U was added to a pre-cleaned Teflon beaker, spiked with the U double-spike, left to equilibrate on a hotplate before being dried down at 100 °C. The sample was then re-dissolved in 5 ml 7 N HCl in preparation for column chromatography.

2.4. Column chromatography

A one step purification and U–Mo separation procedure was conducted using RE Resin (Triskem technologies) in custom-made shrink-fit Teflon columns (~0.2 ml resin reservoir). Prior to sample loading, resin was added to the columns, pre-cleaned using 2 ml of a mixture 0.1 N HCl–0.3 N HF, rinsed with MQ water, and pre-conditioned with 2 ml 7 N HCl. Samples were then loaded in 5 ml 7 N HCl and the matrix eluted with 10 ml 1 N HCl. The Mo and U fraction were eluted separately, first with 5 ml 0.2 N HCl and then 5 ml of a 0.1 N HCl–0.3 N HF mixture, respectively. The column chromatography protocol yielded highly pure Mo and U fractions with only traces of major or minor elements. For example, abundant cations in the pre-column extracted seawater – e.g. Mg (~1000 ppm) and Ca (~400 ppm) – were present at less than 100 ppb in the purified Mo and U fractions. Column blanks were <13 pg and <22 pg for Mo and U, respectively (Supplementary Table 1). The U fractions were fluxed on a hotplate for 24 hours in a 1 ml mixture of concentrated HNO_3 and H_2O_2 in 1:1 ratio, to oxidise any resin bleeding into the sample cut during chemistry, and dried down. The purified Mo and U were then re-dissolved in 0.3 N HNO_3 and 0.2 N HCl, respectively, for mass spectrometry.

The column separation procedure was tested by processing two open Atlantic Ocean samples for U and Mo, following the dissolution and column chemistry procedure described above. The isotopic compositions of Mo and U measured are in good agreement with previously reported values (see below and Supplementary Table 1) (Siebert et al., 2003; Weyer et al., 2008; Nakagawa et al., 2012; Andersen et al., 2014; Tissot and Dauphas, 2015).

2.5. Elemental concentration measurements

The concentrations of selected elements (see Supplementary Table 2) were measured in 0.3N HNO_3 using a Thermo–Finnigan Element XR ICP–MS, following the same measurement

protocol as outlined in Andersen et al. (2013, 2016). In brief, the instrument set-up included both low and medium resolution, using a primary in-house concentration standard interspersed with measurements of three unknowns and a secondary standard (BCR–2). The BCR–2 standard was used to monitor the accuracy and reproducibility. Repeated measurements of BCR–2 gave a reproducibility better than ± 10% (1 S.D.) and mean values within ± 10% of the certified concentrations (see Andersen et al., 2016).

2.6. Molybdenum and uranium isotope measurements

Isotope ratios were measured on a Neptune (Thermo–Finnigan) MC–ICPMS equipped with an AridusII auto-sampler (CETAC) using a PFA nebulizer and spray chamber (CPI) sample introduction system. Details of instrumental set-up are given in Archer and Vance (2008) for Mo isotopes and Andersen et al. (2016) for U isotopes. Molybdenum isotope ratios are presented as $\delta^{98}Mo = [^{98/95}Mo_{sample}/^{98/95}Mo_{standard} - 1] \times 1000$. All Mo isotope compositions for samples are reported relative to NIST SRM 3134 = +0.25‰ (Nägler et al., 2014). Uranium isotope ratios are reported relative to the CRM–145 standard and presented as $\delta^{238}U = [^{238/235}U_{sample}/^{238/235}U_{standard} - 1] \times 1000$ and as ($^{234}U/^{238}U$) activity ratios compared to secular equilibrium (Cheng et al., 2013).

The Mo double spike method was verified via the analysis of an in-house CPI standard as well as open-ocean seawater. During the period of this study, analysis of our in-house CPI standard with standard/spike ratios in the range of 0.1 to 5 gave $\delta^{98}Mo = -0.02 \pm 0.04$‰ (all isotope data reported as 2 S.D., Supplementary Table 1) relative to NIST SRM 3134 = +0.25‰. Four seawater samples gave $\delta^{98}Mo$ of +2.37 ± 0.03‰, in perfect agreement with previous data for seawater $\delta^{98}Mo$ (Siebert et al., 2003; Nakagawa et al., 2012). The verification of the U double spike method was carried out via repeated measurements of the in-house CZ–1 uraninite

standard and five open-ocean seawater samples (Supplementary Table 1). The long-term average and ±2 S.D. reproducibility for the CZ–1 standard were –0.04 ± 0.07‰ for $\delta^{238}U$ and 0.9996 ± 0.0025 for ($^{234}U/^{238}U$) (Supplementary Table 1), in agreement with previously reported values (Stirling et al., 2007; Andersen et al., 2015; 2016). Uranium isotopic analysis of five seawater samples gave a $\delta^{238}U$ = –0.39 ± 0.04‰ and ($^{234}U/^{238}U$) = 1.147 ± 0.003, again in very good agreement with reported data for seawater (Weyer et al., 2008; Andersen et al., 2010; 2014; Tissot and Dauphas, 2015). Finally, a set-up measuring samples with low U (2–10 ng) amounts equivalent to some filter samples, yielded $\delta^{238}U$ = –0.02 ± 0.23‰ and ($^{234}U/^{238}U$) = 0.999 ± 0.018 for the CZ–1 standard (Supplementary Table 1).

3. Results

3.1. General chemical characterisation of the water column

Salinity, oxygen ($[O_2]$), sulfide ($[\Sigma S^{-II}]$), particulate Fe ($[Fe]_{part}$) and particulate Mn ($[Mn]_{part}$) in the water column are presented in Supplementary Table 2 and summarised in Figure 1. During the study period (2013 and 2015) the lowest salinity recorded was during winter and spring due to increased precipitation and decreased evaporation during the colder season of the year. The position of the halocline is temporally variable, from approx 5 to 9 m. Oxygen concentrations are strongly inversely correlated with the $[\Sigma S^{-II}]$, the latter reaching the highest concentration of ~5 mmol l^{-1} in summer 2013 at 13 m depth. Particulate Fe and Mn are higher at the chemocline and in the deeper anoxic waters than in the upper oxic layer.

3.2. Molybdenum in the water column and settling particles

Depth profiles of salinity-normalised (to 35) dissolved Mo ($[Mo]_{SNdiss}$) and of particulate Mo ($[Mo]_{part}$), as well as their $\delta^{98}Mo$, are presented in Supplementary Table 2 and Figure 2. The

$[Mo]_{SNdiss}$ is higher than the measured [Mo] by 3 to 50% in the upper oxic waters (O_2 > 5 mg l^{-1}) that are influenced by precipitation, but the correction has little impact on the deeper anoxic waters. The $[Mo]_{SNdiss}$ profiles show a strong depth gradient, mirroring changes in the redox conditions in the water column. With the exception of very high [Mo] in surface waters in April and July 2013, [Mo] generally varies between ~100 nmol l^{-1} in the oxic and ~10 nmol l^{-1} in the deeper euxinic waters. The shape of the profiles is rather different for the first three sampling dates (February-July 2013) versus the last three (Oct 2013, April 2015, July 2015). The latter three profiles show a much sharper transition across the chemocline and much more homogeneous concentrations within each redox regime – the upper oxic layer and the lower euxinic layer. For the later three sampling times, $[Mo]_{part}/[Mo]_{diss}$ is homogeneously low in the upper oxic water column (generally ≤0.01) and higher in the lower anoxic portion (up to 0.19). The first three sampling events are also much more heterogeneous in this ratio.

Lake Rogoznica waters generally show dissolved Mo isotopic composition ($\delta^{98}Mo_{diss}$) in the range +2.2 to +2.5 ‰ (Fig. 2). The exception is April 2013 and the top of the water column in July 2013, where values are much more variable and extend down to +0.8‰. The isotopic composition of the particulate Mo ($\delta^{98}Mo_{part}$) spans a wide range, from $\delta^{98}Mo$ = +0.1 to +2.1‰. In the anoxic water column the particles were generally more enriched in heavy Mo isotopes ($\delta^{98}Mo_{part}$ from +0.6 to +2.0‰) in comparison with those from the oxic water column (from +0.1 to +1.8‰).

3.3. Uranium in the water column and settling particles

Salinity normalised ($[U]_{SNdiss}$) and particulate ($[U]_{part}$) U concentrations, as well as $\delta^{238}U$, are presented in Supplementary Table 3 and Figure 2. As with Mo, the salinity normalisation increases the $[U]_{SNdiss}$ by 2 to 50% in the upper oxic waters influenced by precipitation, but has

little influence on the deeper high salinity anoxic waters. The deeper anoxic waters are depleted in dissolved U ($[U]_{diss}$: 1.4 to 3.4 nmol l^{-1}) compared to the oxic surface layer (8.9 to 11.2 nmol l^{-1}). Dissolved [U] decreases towards the bottom for all 6 sampling campaigns. Particulate U concentrations (normalised to the water volume the filters were extracted from) are generally low, ranging from 0.01 to 0.1 nmol l^{-1} during the whole sampling period, and show no significant seasonal variation. Particulate U concentrations are consistently higher within the anoxic waters column, reaching a maximum at the chemocline and the bottom of the lake. The $[U]_{part}/[U]_{diss}$ is significantly lower than the $[Mo]_{part}/[Mo]_{diss}$ ratio, reaching max values of 0.004 for the oxic water column and 0.03 for anoxic water column samples.

Data for the uranium isotopic composition of the dissolved pool ($\delta^{238}U_{diss}$) show lighter values than that for open-ocean seawater ($\delta^{238}U$ = -0.39‰, Supplementary Table 1), ranging from –0.5 to –1.1‰ and with generally lower values with depth. The isotopic composition of particulate U ($\delta^{238}U_{part}$) is in the range –0.2‰ to –1.5‰, with the lowest $\delta^{238}U_{part}$ recorded in July 2013 at 6m depth, near the chemocline. $(^{234}U/^{238}U)_{diss}$ was in the range 1.111 to 1.148 and $(^{234}U/^{238}U)_{part}$ in the range 1.101 to 1.152 (Supplementary Table 3).

3.4. Molybdenum and uranium in the sediments and pore water

Mo and U concentrations ($[Mo]_{bulk}$, $[U]_{bulk}$) and isotopic compositions ($\delta^{98}Mo_{bulk}$, $\delta^{238}U_{bulk}$) in the anoxic sediments are presented in Supplementary Table 4 and Fig. 3. These bulk data were used to calculate authigenic abundances using the measured Al, Mo and U in the sediment samples (Supplementary Table 4) and assumed lithogenic Mo/Al and U/Al ratios of 1.1×10^{-5} g g^{-1} and 1.8×10^{-5} g g^{-1}, respectively (Taylor and McLennan, 1985; Tribovillard et al., 2006; Andersen et al., 2014). For the isotopic composition of the detrital component a

$\delta^{98}Mo_{det}$ of +0.3‰ (Voegelin et al., 2014) and a $\delta^{238}U_{det}$ of -0.3‰ (Andersen et al., 2016), were used, with:

$$\delta^{98}Mo_{auth} = \frac{(\delta^{98}Mo_{bulk}[Mo]_{bulk} - \delta^{98}Mo_{det}[Mo]_{det})}{[Mo]_{auth}} \quad [1]$$

$$\delta^{238}U_{auth} = \frac{(\delta^{238}U_{bulk}[U]_{bulk} - \delta^{238}U_{det}[U]_{det})}{[U]_{auth}} \quad [2]$$

Using this approach, the detrital Mo contribution to the sedimentary budget is found to be minimal, so that more than 99% of the Mo in the sediments has an authigenic origin. Thus, the impact of the detrital fraction on the measured bulk Mo isotopic composition of the sediment is also negligible. For the bulk U there is a higher contribution of detrital U (from 10 to 23%). Accordingly, the calculated authigenic $\delta^{238}U$ is shifted towards slightly lower values (by up to 0.03‰) relative to the bulk sediment. The measured ($^{234}U/^{238}U$) ratio in the samples, along with an assumption that the detrital material is in secular equilibrium (~1) and that the authigenic U has a ratio = 1.147 like modern seawater, provides an alternative method for performing the detrital U correction. The sediments display high ($^{234}U/^{238}U$), ranging from 1.096 to 1.120, demonstrating the predominance of authigenic U. Removal of the detrital U component from the bulk using ($^{234}U/^{238}U$), leads to corrected $\delta^{238}U$ authigenic values that are essentially the same as those obtained using the U/Al method (see Supplementary Table 4).

The $[Mo]_{auth}$ and $[U]_{auth}$ were in the range 11 to 80 μg g^{-1} and 2.4 to 7.3 μg g^{-1}, respectively, implying moderate Mo and U enrichments in the anoxic sediments. The $\delta^{98}Mo_{auth}$ is variable (1.6 to 2.2‰), but is consistently lower than the average oceanic $\delta^{98}Mo$

composition (+2.36 ± 0.10‰, Siebert et al., 2003). Sedimentary $\delta^{238}U_{auth}$ is, on average, slightly higher (~0.15‰) than the average oceanic $\delta^{238}U$ (–0.39‰), with the exception of the sample from 17.5 cm ($\delta^{238}U_{auth}$ = –0.42 ± 0.07‰). The sedimentary ($^{234}U/^{238}U$) shows no significant variability throughout the investigated core (Supplementary Table 4). The measured host carbonate rock sample gave a $\delta^{238}U$ = –0.16 ± 0.04‰, a ($^{234}U/^{238}U$) of 1.012, a $[U]_{bulk}$ of 1.12 µg g^{-1} and $[Mo]_{bulk}$ of 0.72 µg g^{-1} (Supplementary Table 4).

Pore water Mo and U concentrations ($[Mo]_{pw}$, $[U]_{pw}$) (Supplementary Table 5, Fig. 3) were consistently low throughout the core, with average $[Mo]_{pw}$= 5 ± 1 nmol l^{-1} and $[U]_{pw}$ = 0.17 ± 0.04 nmol l^{-1} (n=13). The $\delta^{238}U_{pw}$ closely resembles the $\delta^{238}U_{diss}$ recorded in the deepest anoxic bottom waters ($\delta^{238}U_{diss}$ in the range –0.9 to –1.1‰). In contrast, pore water Mo is slightly enriched in the heavier Mo isotopes, with an average $\delta^{98}Mo_{pw}$ of +2.48 ± 0.08‰ (n=13), in comparison to $\delta^{98}Mo_{diss}$ in anoxic bottom waters (see Figures 2 and 3).

4. Discussion

4.1 Behaviour of Mo and its isotopes in Lake Rogoznica

4.1.1 Water column Mo behaviour

The depth profiles for Mo and its isotopes in Fig. 2 split into two types of behaviour. The dissolved Mo concentration profiles for October 2013 to July 2015 closely resemble those previously reported from Lake Rogoznica (Helz et al., 2011), in showing a sharp transition across the chemocline from high in the oxic portion above to low in the anoxic part of the lake below. Profiles between Feb 2013 and July 2013, on the other hand, show more unexpected behaviour. Below we discuss these anomalous features first, before moving on to the more "typical" features of the later three sampling campaigns.

The first three sampling campaigns, and in particular April and July 2013, are often characterised by very high Mo concentrations ($[Mo]_{SN}$ up to 577 nmol l^{-1}) in oxic surface waters. (Fig. 2). Moreover, although these profiles exhibit the expected decrease of dissolved Mo in anoxic waters, concentrations at depth are up to 2.5 times higher than in the later three sampling campaigns. These high dissolved Mo concentrations are associated with generally lower $\delta^{98}Mo_{diss}$, both in the oxic upper water column (as low as +0.75 ± 0.02‰) and in the deep euxinic portion (as low as +1.32 ± 0.02‰). Combined, these observations suggest an additional source of isotopically light Mo to the water column before or during this period. For the oxic part of the water column, the Mo abundance and isotopic data are mostly explained by the mixing of a "normal" signature, typified by the analyses from October 2013 to July 2015, with an additional Mo source that has a $\delta^{98}Mo$ of around +0.4 to +0.5‰ (Fig. 4a).

The origin of this additional Mo source is more difficult to identify. The Mediterranean generally sees unusually high dust supply from the Sahara (Prospero, 1996), and one possibility is that the additional Mo derives from such a source. The Mo associated with dust is most likely to be associated with Fe-Mn oxyhydroxide-rich surfaces, which have the required light isotope compositions (e.g. Barling and Anbar, 2004; Goldberg et al., 2009). It is notable that the reservoir of Mo in particulates is also high, by one or two orders of magnitude, during the anomalous sampling periods. The $\delta^{98}Mo_{part}$ is also consistently lower than during the last three sampling campaigns, particularly in the upper oxic water column where the difference between the dissolved and particulate loads ($\Delta^{98}Mo_{diss\text{-}part}$) is up to +2.2‰ in the first three samplings versus a maximum of +1.3‰ in the second three. The suggested dust source is not strongly supported by particulate Al, Fe and Mn concentrations which, though variable through time and space, are not particularly strongly correlated with high Mo concentrations or light Mo isotopes. On the other hand, if dust particles fall quickly through the water column while their impact lingers in the dissolved pool, or if Mo on Fe-Mn

coatings is particularly soluble relative to Fe and Mn, such a correlation might not necessarily be expected.

Another potential Mo source could, in principle, be leaching of Mo from the surrounding carbonate karst. However, Mo concentration in the carbonate rock sample measured was low (0.71 μg g^{-1}, Supplementary Table 4), in agreement with previously reported values for carbonate (Vogelin et al., 2009, 2010). The main reservoir of Mo in the carbonate host rock is also likely to be Fe-Mn oxyhydroxide coatings. The vertical position of the halocline in Lake Rogoznica shifts seasonally, and during winter 2013 it was situated at a relatively shallow level (3 to 4 m depth). This may have allowed anoxic waters to enter into karst channels and dissolve Fe-Mn oxyhydroxide coatings on carbonate. Finally, the vertical position of the chemocline in Lake Rogoznica also varies, by 2-4m, again depending on season and meteorological conditions. Such temporal variation may also periodically expose Mo sequestered to Fe-Mn oxyhydroxides, in recently deposited unconsolidated sediment in the oxic portion of the lake, to reductive dissolution.

During the last three sampling campaigns dissolved salinity-normalised Mo concentrations in the upper 5m of the water column are, at 97±5 nmol kg^{-1}, close to the mean oceanic $[Mo]_{diss}$ value (107 ± 7 nmol l^{-1}, Collier, 1985; Nakagawa et al., 2012). In addition, the average $\delta^{98}Mo_{diss}$ for these samples is +2.16 to 2.34‰, similar to the measured average oceanic dissolved pool $\delta^{98}Mo$ signature ($\delta^{98}Mo$= +2.37 ± 0.03‰, Supplementary Table 1). The $\delta^{98}Mo_{part}$ ranged from +0.98 to +1.68‰ in the oxic surface waters and $\delta^{98}Mo_{diss\text{-}part}$ = 0.65-1.53‰. This difference is consistent with a dominant role for amorphous Fe (oxyhydr)oxides (e.g. ferrihydrite, goethite), which have been shown experimentally to exhibit fractionations relative to dissolved Mo in the range of 1.1 to 1.4‰ (Goldberg et al., 2009).

At the chemocline, $[Mo]_{diss}$ decreases and reaches steady concentrations of about 9 nmol l^{-1} in the anoxic (O_2~0 mg l^{-1}) waters below, a behaviour previously observed both at Lake Rogoznica (Helz et al., 2011), and in other modern euxinic basins (Emerson and Huested, 1991; Colodner et al., 1995; Algeo and Tribovillard, 2009; Nägler et al., 2011). In all the profiles there are minor but significant excursions in $\delta^{98}Mo$ of the dissolved pool close to the chemocline. For example, in October 2013 and April 2015, $\delta^{98}Mo_{diss}$ shows a slight increase, by about 0.3‰, just at and below the chemocline and at depths where significant removal of dissolved Mo starts. Just beneath this, $\delta^{98}Mo_{diss}$ decreases again and the deepest samples are again close to those in oxic waters, at $\delta^{98}Mo_{diss}$ = +2.31±0.14‰. The July 2015 campaign does not record the initial increase as Mo concentrations begin to drop with depth. Particulate Mo concentrations increase beneath the chemocline, and though they stay beneath 2 nmol l^{-1}, the $[Mo]_{part}/[Mo]_{diss}$ ratio increases to values as high as 0.2. The $\Delta^{98}Mo_{diss\text{-}part}$ decreases with depth, with $\delta^{98}Mo_{part}$ compositions up to +2.03‰ in the deeper anoxic water column.

To our knowledge, the only other study reporting $\delta^{98}Mo$ values for sinking particles formed in anoxic water columns is that for Lake Cadagno, Switzerland, in Dahl et al. (2010). This study hypothesised that $\Delta^{98}Mo_{diss\text{-}part}$ in anoxic waters is a function of both $[H_2S]_{aq}$ and the time available for equilibration between particles and water versus the scavenging lifetimes of intermediate thiomolybdate species. In this view, when sulfide levels are low enough for non-quantitative transformation of molybdate to tetrathiomolybdate, and for rapid scavenging timescales for intermediate thiomolybdate species, isotopic differences are expected between residual dissolved Mo and particulate Mo (Tossell, 2005; Kerl et al., 2017).

Consistent with this view, the data for $\Delta^{98}Mo_{diss\text{-}part}$ within the water column of Lake Rogoznica does exhibit a strong relationship with total dissolved sulfide (Fig. 4b). But the relationship appears to become asymptotic to a value of about +0.3‰ at very high dissolved sulfide levels. It is possible that general conclusions regarding the behaviour of Mo and its isotopes in euxinic water columns from these Lake Rogoznica data are complicated by the potential impact of Fe-Mn oxyhydroxide particulates, discussed earlier with reference to the first three sampling campaigns. For example, it is possible that the small excursions near the chemocline could be caused by oxidative-reductive cycle involving Fe-Mn oxyhydroxides. Such a rationale is not, however, consistent with all the details of the data. Thus, the small increase in $\delta^{98}Mo_{diss}$ just below the chemocline, where Mo is first removed from the water column, is the opposite to that which might be expected if isotopically light Fe-Mn oxyhydroxides were sinking into the euxinic layer and undergoing reductive dissolution. Rather this feature, coupled to increases in the Mo_{part}/Mo_{diss} ratio, is much more readily explained in terms of preferential and non-quantitative removal of light Mo isotopes to particulates due to formation of intermediate thiomolybdates at low dissolved sulfide concentrations. Thus, although the exact value of $\Delta^{98}Mo_{diss\text{-}part}$ in the anoxic water column is difficult to estimate from our data set, it is very likely that the removal of Mo from the anoxic water of Lake Rogoznica is associated with minor Mo isotope fractionation, similar to that already observed in Kyllaren Fjord, Black and Baltic Sea anoxic water columns (Nägler et al., 2011; Noordmann et al., 2015).

4.1.2 Mo and its isotopes in sediment and pore water

As noted in Section 3, the detrital Mo component of anoxic Lake Rogoznica sediments is very small, and more than 99% has an authigenic origin. The overall $\delta^{98}Mo_{auth}$ is high (Fig. 3), ranging from +1.6 to +2.2‰, and with an average of 1.95 ± 0.17‰, (n=13, 1SD). The

dissolved-particulate difference for sediment-pore water pairs shows a more scattered relationship with total dissolved sulfide than data for the water column (Fig. 4b). It is again the case, however, that $\Delta^{98}Mo_{diss\text{-}part}$ is never zero, and the minimum values observed are again about 0.3‰, similar to the water column. This overall finding is again consistent with the previous suggestion in Nägler et al. (2011) that $\Delta^{98}Mo_{diss\text{-}part}$, even for near-quantitative removal to sediment at high sulfide concentrations, does involve a small fractionation.

On the other hand, sediments at Lake Rogoznica are again more complicated than such a simple picture can explain. Dissolved sulfide levels in the pore waters of Lake Rogoznica are very high, and equilibration times in the sediment are presumably long. Thus, the occasionally high values of $\Delta^{98}Mo_{diss\text{-}part}$ are difficult to explain without invoking some temporal variation in redox conditions. Most of the time, Lake Rogoznica waters are characterised by a sharp chemical gradient and an anoxic layer with high $[H_2S]_{aq}$ at depths >8–9 m, but seasonal mixing is known to occur during particularly dry and cold autumn periods (Ciglenečki et al., 2005; Helz et al., 2011; Ciglenečki et al., 2015). During these periods cold oxygenated waters slowly sink towards the bottom, causing contraction of the anoxic layer so that anoxic conditions are restricted to the deep nepheloid layer (~13 m, Helz et al., 2011). The last two such complete mixing events occurred in 2011 and 1997 (Ciglenečki et al., 2005; Ciglenečki et al., 2015). After these events, anoxia is re-established, potentially causing reductive dissolution of Fe-Mn (oxyhydr)oxides deposited at the bottom of the lake during mixing events (Helz et al., 2011). We speculate that, after these events, Lake Rogoznica bottom waters are most probably enriched in light Mo isotopes, which could potentially affect the isotopic composition of Mo extracted from such waters.

4.2 Behaviour of U and its isotopes in Lake Rogoznica

4.2.1 Uranium and its isotopes in the water column

Previous studies from the two major modern semi-restricted euxinic basins (Cariaco Basin and Black Sea) have suggested that in such settings U is not removed to sediment through processes in the water column, but rather via reduction in sediment driving U diffusion from the overlying waters into the sediments (Anderson, 1987; Anderson et al., 1989a). The first-order features of the Lake Rogoznica data can first be assessed in terms of this paradigm, in the interests of ascertaining whether it is generally applicable to euxinic basins of different sizes and, for example, at the very high dissolved sulfide concentrations seen in Lake Rogoznica.

Focusing first on U concentration, the above scenario implies no removal term in the water column, so that water column depth profiles should be explained in terms of diffusion and advection processes alone. In a simplified diffusion-advection-reaction framework the precise shapes of [U] depth profiles will be dependent on the rate of U diffusion into sediment compared to the rate at which the water column is mixed by advection. Here we assess whether such a simplified model explains the first order features of the [U] data for Lake Rogoznica.

At steady-state, any depth profile in the lake can be modelled using the ADR equation:

$$D_z \frac{d^2C}{dz^2} - \omega_z \frac{dC}{dz} - kC = 0 \qquad [3]$$

where z is depth, D is the rate of diffusion, ω is the rate of advection and k is a rate constant for removal *within* the water column. If there is no removal within the water column (k = 0), the solution to equation [3] for boundary conditions $C(z) = C_0$ at z = 0 (lake surface) and $C(z) = C_m$ at z = m (lake bottom) is:

$$C(z) = C_0 + (C_m - C_0)\frac{e^{\frac{\omega_z}{D_z}z} - 1}{e^{\frac{\omega_z}{D_z}z_m} - 1} \quad [4]$$

By setting suitable [U] at the top (C_0) and bottom (C_m), model depth profiles can be compared to the data.

The depth profiles for [U] from the different sampling campaigns (Fig. 2,5A) vary between those that are close to continuous U depletion profiles with increasing depth (diffusion-dominated), versus others suggesting a very strong chemocline separating well-mixed upper and lower layers (advection dominated within each layer, diffusion across the chemocline). For example, the entire [U] depth profiles from the early sampling campaigns (e.g. February 2013) can be modelled in terms of processes dominated by diffusion downwards into the sediment (Fig. 5), with no requirement for removal or addition (no reaction term) within the water column. The later sampling campaigns, where a more stratified water column develops, better approximate to two well-mixed reservoirs above and below the chemocline, with more limited mass transfer between (e.g. July 2015; Fig. 5). This type of profile requires advective mixing within the upper and lower layer, coupled to slower diffusive transport across the chemocline, but is also completely consistent with the lack of a removal term within the water column.

Overall, then, the first order features for the water-column dissolved pool uranium concentrations require no removal within the water column, consistent with earlier conclusions for the Black Sea and Cariaco Basin that U removal occurs within sulfidic sediments (Anderson, 1987; Anderson et al., 1989a). Further, more detailed, constraints on the U removal process come from water column U isotopes. Uranium isotope fractionation occurs during the U(VI) to U(IV) transition, as evidenced by theoretical equilibrium calculations (e.g. Bigeleisen 1996) and abiotic and biotic experiments (e.g. Basu et al., 2014; Stylo et al., 2015; Stirling et al., 2015;

Wang et al., 2015). The overall isotope fractionation associated with uranium reduction is about 1-1.3 ‰, with the heavy isotope preferred in the reduced species (e.g. Bigeleisen, 1996; Fujii et al., 2006; Abe et al., 2008, 2010). In the modern euxinic Black Sea, $\delta^{238}U$ in sediments is generally around 0.4 ‰ higher than the open ocean value, while the deeper water column is driven to lower $\delta^{238}U$ (Weyer et al. 2008; Andersen et al. 2014; Rolison et al. 2017). Previously (Andersen et al. 2014) these data were explained in terms of an effective U isotope fractionation of +0.6‰, i.e. about half the full fractionation, due to U uptake and precipitation in sediments driven by diffusion from overlying seawater and transport-diffusion limitation in the pore water-sediment (e.g. Bender, 1990; Clark and Johnson 2008).

If U removal occurs in this manner, the faster removal of ^{238}U than ^{235}U into the sediment should lead to systematically lower $\delta^{238}U$ in the waters above and must occur in a manner that is consistent with the 0.6‰ difference in the sequestration of ^{238}U relative to ^{235}U (see supplementary text for details). On the other hand, if U were to be removed via reduction in the water column itself with no transport-diffusion limitation, the U isotope fractionation process is expected to produce water column $\delta^{238}U$ values that reflect the full ~1.2 ‰ fractionation. At steady state, the overall input of U and its isotopes to Lake Rogoznica from the open sea must equal the outputs, i.e. outflow of water from the lake to the ocean, and output to sediment:

$$C^{ocean}F_{exch} - C^{lake}F_{exch} - kC^{lake} = 0 \qquad [5]$$

Where C^x is [U] in the ocean or lake, F_{exch} is the water exchange rate and k is a rate constant for removal of U to sediment. Rearranging:

$$C^{lake} = F_{exch}\frac{\left(C^{ocean} - C^{lake}\right)}{k} \qquad [6a]$$

The above is also true for each of ^{238}U and ^{235}U so that:

$$C^{lake}_{238} = F_{exch}\frac{\left(C^{ocean}_{238} - C^{lake}_{238}\right)}{k_{238}} \quad \text{and} \quad C^{lake}_{235} = F_{exch}\frac{\left(C^{ocean}_{235} - C^{lake}_{235}\right)}{k_{235}} \qquad [6b]$$

Combining [6a] and [6b]:

$$\frac{C^{lake}_{238}}{C^{lake}_{235}} = \frac{k_{235}}{k_{238}}\left(\frac{C^{ocean}_{238} - C^{lake}_{238}}{C^{ocean}_{235} - C^{lake}_{235}}\right) \qquad [7]$$

Thus, at steady state the average $^{238}U/^{235}U$ ratio of the lake is independent of the relative sizes of the uranium fluxes, and depends only on the isotopic composition of the output to sediment and the degree to which the lake water is modified between input and output.

For Lake Rogoznica, potential scenarios can be examined with the above model of steady state U removal and the $\delta^{238}U$ vs [U] systematics (Fig. 6). The ultimate input of U may be approximated by the open ocean, with $\delta^{238}U$ of -0.4 ‰ and [U] of 13.4 nM. Though this may be slightly modified during transport through the karst, the ($^{234}U/^{238}U$) in the lake water is close to the open ocean value, suggesting this effect is minor. Fig. 6 shows all the water column data for all sampling campaigns. Clearly, though the data lie closer to the diffusion-driven U removal model (solid line in Fig 6A, $k_{235}/k_{238} = 0.9994$) than one involving irreversible removal in the

water column (dashed line in Fig 6A, k_{235}/k_{238} = 0.9988), there is also considerable scatter. Some of this scatter is, however, readily explainable once more in terms of the relative importance of diffusion and advection, with little requirement for reaction within the water column. Thus, for example, data for February 2013 again approximate most closely a situation where diffusion occurs into the sediment across the whole depthscale of the lake (Fig. 6A). But where stratification of the lake occurs, again typified by July 2015 (Fig. 6C), it is only the lower anoxic portion of the lake that approximates the model for diffusion into sediment, whereas the well-mixed upper portion of the lake, now isolated from the sediment by the strong chemocline, shows a more homogeneous U isotopic composition much closer to the oceanic input.

The depth profiles for the U isotope data in Fig. 2 clearly point to further minor processes, especially near the chemocline. For example, there is clear but minor isotope exchange with particulate material in July 2013 (Fig. 2) when the dissolved U pool situated just above the chemocline was isotopically light, probably due to the degradation of particulate organic matter with isotopically light U, similar to observed in sediment traps from Saanich Inlet (Holmden et al., 2015). But the above discussion clearly suggests that the first-order process governing U removal at Lake Rogoznica, in common with the Black Sea and despite the higher water column sulfide concentrations, is via U diffusion downward into sediments followed by reductive U precipitation with a net U isotope fractionation of +0.6‰. The dominance of this first–order U removal process should, therefore, be reflected in the authigenic U and its isotope composition imprinted on the sediment.

4.2.2 Mass balance for U and its isotopes in the lake system

In principle, a diffusive removal flux for U can be calculated if the depth of U removal in the pore-waters is known (e.g. Bender, 1990). This estimate could establish whether the U diffusion

rate across the sediment-water interface rate is fast enough to account for the observed U accumulation rate in the sediments. However, the pore water data at hand are not at high enough resolution to allow this calculation – the required diffusive flux dictates an e-folding lengthscale for pore water removal of about 0.2 cm. On the other hand, the U isotope composition of the accumulated authigenic U should reflect that dictated by the diffusive U flux model if this represents the main U removal term. Thus, the $^{238}U/^{235}U$ of authigenic U in sediment is expected to be ~0.6‰ heavier than the overlying bottom waters (see supplementary text). At Lake Rogoznica, the average $\delta^{238}U$ of bottom waters for the six sampling campaigns is -0.94±0.07‰ (1SD), while the average authigenic sediment composition is -0.30±0.07‰ (1SD). The difference is in good agreement with the diffusion-driven removal scenario, confirming this process as the main U removal mechanism.

In general, if U is to be removed by the U diffusion process from an infinitely large (or rapidly replenished) water column with an open ocean composition (-0.4‰) the $\delta^{238}U$ of authigenic U is expected to be ~+0.2‰. At the other extreme, if the U removal flux is significantly larger than the replenishment rate, thus fully depleting the water column in U, sedimentary authigenic U should equal the input. These systematics reflect the degree of restriction of the system, and are explored in Fig. 7 for Rogoznica and other semi-restricted anoxic basins for which data are available (Kyllaren Fjord, Black Sea, Saanich Inlet, Cariaco Basin, see Table 1). Fig. 7 highlights a clear relationship between the U concentration in the lake bottom waters with the authigenic $\delta^{238}U$ in the sediments (open symbols and blue line). This suggests that the dominant U removal mechanism - U diffusion and reduction within the sediments - was the same in each semi-restricted basin. This includes the Saanich Inlet, in contrast to a previous study (Anderson et al. 1989b) that suggested that the diffusive removal U flux was of insufficient size to be the dominant source of authigenic U in the sediments. However, this latter U removal flux estimate, based on one pore water profile in the anoxic part of the inlet, may have been underestimated

due to a lack of representativeness of this one profile or to artifacts during U porewater extraction. A shallow pore water depletion profile of ~0.5 cm (Anderson et al 1989b), similar to that indicated for Lake Rogoznica, would be required for the diffusive U flux to be the dominant U removal process in Saanich Inlet. If the diffusive U flux had indeed been underestimated, this would explain the similarities between authigenic U isotope data in Saanich Inlet sediments (Holmden et al., 2015) and those for other semi-restricted basins, where the diffusive removal process has been shown to be dominant (Figure 7). There is also a reasonably good correlation between authigenic $\delta^{238}U$ and water column sulfide concentrations (closed symbols, red line). If U removal is driven by diffusion into sediment, a mechanistic correlation with the reduction potential of S^- is not expected. But this correlation may be a more-or-less co-incidental consequence of the control that deepwater overturning timescales exert on both sulfide concentrations and authigenic $\delta^{238}U$. Relatively fast water overturning rates would lead to less S^- buildup in the water column, replenishment of U in the water column, and authigenic $\delta^{238}U$ fractionated from open ocean seawater. In contrast, relatively slow deepwater renewal rates may lead to higher S^-, slower U replenishment rates, more quantitative removal of U from the water column and authigenic $\delta^{238}U$ less fractionated from open ocean seawater.

4.3. Mass balance for U, Mo and their isotopes in Lake Rogoznica and other euxinic basins

The impact of deep water renewal rates on sediment geochemistry can be further explored in the context of coupled sedimentary U and Mo concentrations and isotope systematics (Fig. 8). The key difference between Mo and U is the removal mechanism in a euxinic water column, with U driven by diffusion from the water column into sediment where it is fixed, while Mo is scavenged by particulate material in the water column and transported to the sediment in solid form. These different removal mechanisms have been used to fingerprint specific redox conditions using coupled U vs. Mo enrichment systematics in sediment (e.g. Algeo and

Tribovillard, 2009). Thus, in a closed system where Mo and U are quantitatively removed, the Mo/U ratio and the Mo and U isotope composition of the sediment should equal the input from the open ocean. Such behaviour is rarely the case, however, with different euxinic basins showing variable Mo/U ratios and Mo and U isotope compositions (Fig. 8). Of the euxinic basins with Mo and U isotope data, only Kyllaren Fjord (Noordmann et al., 2015) shows Mo/U ratios and Mo and U isotope compositions close to the open ocean, indicating near quantitative uptake of both Mo and U. Sediments from the deepest part of the Black Sea (Station 9 with both U and Mo isotope data; Arnold et al., 2004; Andersen et al., 2014) show a Mo/U ratio significantly below the seawater value (see also Tribovillard et al., 2006; Algeo and Tribovillard, 2009). This behaviour has been linked to the contrasting sedimentary output mechanisms for Mo and U, and the fact that the Black Sea exhibits extreme stratification and long deep water renewal times (>500 years; Algeo & Lyons, 2006), leading to deep water Mo depletion from slow resupply (Algeo &Tribovillard, 2009).

At Lake Rogoznica, Mo/U ratios are, on average, about twice the seawater value (Fig. 8A). Where this has been reported, including at Saanich Inlet (Russell and Morford, 2001; Holmden et al., 2015; Amini et al., 2016) and in the Cariaco Basin (Arnold et al., 2004; Andersen et al., 2014), it is often interpreted as evidence for Mo addition to sediment via a Fe-Mn oxide "particulate shuttle" (e.g. Algeo and Tribovillard, 2009). This suggestion is supported by the previous documentation of isotopically light Mo in such sediments (Fig 8B), and is also consistent with light Mo isotope data at Lake Rogoznica. It is also true, however, that Mo/U ratios higher than seawater are an expected feature of small reservoirs like Lake Rogoznica, even in the absence of a particulate shuttle, because of the more rapid removal of Mo relative to U from the water column to sediment. In fact, any measurement of the basinal average Mo/U ratio of a euxinic setting must record a Mo/U ratio higher than seawater simply because uranium

will be lost to a greater extent by flow of water out of the basin than will Mo. For a very small and simple reservoir like Lake Rogoznica, and despite uncertainties such as those arising from the possible operation of a Fe-Mn oxide "particulate shuttle", the different removal rates of Mo and U are likely to give higher Mo/U than that of seawater, and this is likely to be recorded in these sediments. Only in the case where the water flow through the euxinic reservoir is so slow that U diffusion into sediment can keep up, will the Mo/U ratio approach the seawater value. In this context, also implicit in the treatment of Algeo and Tribovillard (2009), the Mo/U ratios lower than seawater in the deep, most sulfidic, portion of the Black Sea only arise because of preferential stripping of Mo relative to U from younger - "upstream" - waters.

The Lake Rogoznica isotope data show some similarities to Kyllaren Ford for $\delta^{238}U$, but the low $\delta^{98}Mo$ in both the euxinic waters ($\delta^{98}Mo$ ~2.0-2.4‰) and sediments ($\delta^{98}Mo$ ~1.6-2.2‰), and relatively high Mo/U in the sediments, all seem to require conditions occasionally, though perhaps transient, when isotopically light Mo is added to the basin. The anomalously high [Mo] and low $\delta^{98}Mo$ in April 2013 surface waters, characterised by the lowest $\delta^{98}Mo$ in euxinic waters (~1‰) of any of the sampling campaigns, may have caught one such transient event. However, the arrows on Fig. 8B also indicate schematically how much of the paired Mo-U isotope data for euxinic basins could also be rationalised in terms of (a) variable rates of Mo-U removal relative to each other, possibly driven by variable sulfide concentrations within and between basins, differences in water renewal rates, as well as differences in the ratio of euxinic sediment-water interface (U removal) to volume of euxinic water column (Mo removal); (b) a constant effective $^{238}U/^{235}U$ fractionation factor of about 0.6‰ and; (c) Mo isotope fractionation during the early history of Mo removal, e.g. driven by H_2S concentrations near the action point of switch for complete transformation of $Mo^{VI}O_4^{2-}$ to $Mo^{VI}S_4^{2-}$ (Helz et al., 1996; Tossel et al., 2005; Nägler et al., 2011; Kerl et al., 2017), followed by much more subtle fractionations under the fully euxinic conditions that old waters in the Black Sea encounter (e.g. Nägler et al., 2011).

Though the data for sediments recovered beneath the oldest most sulfide-rich waters of the Black Sea support such a scenario, we currently lack paired U-Mo isotope data from sediments deposited from younger waters to fully test this schematic scenario in the Black Sea.

5. Conclusions

Data presented in this paper for the temporal variation in the marine Lake Rogoznica, for both Mo and U and their isotopes, has permitted a detailed assessment of the behaviour of these redox-sensitive elements in a small euxinic basin, leading to the following principle conclusions.

- Both $\delta^{98}Mo_{part\text{-}diss}$ and $\delta^{98}Mo_{sed\text{-}porewater}$ converge towards a ~0.3‰ offset at high sulfide concentrations, providing further evidence for minor Mo isotope fractionation during non-quantitative Mo uptake into euxinic sediments previously suggested for the Black Sea (Nägler et al. 2011). However, Lake Rogoznica also appears to see periodic addition of significant quantities of isotopically light Mo to the lake waters, possibly from the release of Mo from Fe-Mn oxides formed in the oxic layer.

- Uranium concentration profiles in the lake waters show clear evidence for a dominant mechanism for removal from solution via U diffusion into, and precipitation within, the euxinic sediments. Periods of more intense stratification lead to well-mixed profiles in the oxic upper and euxinic lower layers, with diffusion across the chemocline only. Furthermore, $\delta^{238}U$ in both the sediments and deep water column are consistent with an effective $^{238}U/^{235}U$ fractionation of +0.6‰ during uptake in the sediments, in line with other studied euxinic basins.

- As a result of the different uptake mechanisms of U and Mo it is likely that sediments in different areas of a euxinic basin will show different Mo/U, $\delta^{238}U$ and $\delta^{98}Mo$ systematics. The exact Mo and U patterns represent an interplay between: (i) the size of the basin; (ii) deep water renewal rates; (iii) water-column sulfide concentrations and; (iv) processes related to the Fe-Mn shuttle. This study further emphasises the potential of combined Mo and U systematics to provide a better understanding of the redox conditions reflected in the signatures recorded in ancient sediments.

Acknowledgments

This work was supported by ETH Zürich, the Croatian Science Foundation project IP-11-2013-1205, SPHERE and the European Union Seventh Framework Programme (FP7 2007-2013) under grant agreement n° 291823 Marie Curie FP7-PEOPLE-2011-COFUND (The new International Fellowship Mobility Programme for Experienced Researchers in Croatia - NEWFELPRO), as part of the project "Using lakes to develop isotopic tools for understanding ocean redox through Earth history (IsotopicRedoxTools)". GFdS is supported by a Marie Skłodowska-Curie Research Fellowship under EU Horizon2020 (SOSiC; GA #708407). We would like to thank the editor, C. Holmden and two anonymous reviewers for constructive comments on a previous version of the manuscript.

References

Abe, M., Suzuki, T., Fujii, Y., Hada, M., Hirao, K., 2008. An ab initio molecular orbital study of the nuclear volume effects in uranium isotope fractionations. *J. Chem. Phys.***129**, 164309.

Algeo, T.J. and Lyons, T.W. (2006) Mo-total organic carbon covariation in modern anoxic marine environments: implications for analysis of paleoredox and paleohydrographic conditions. *Paleoceaonography* **21**, 10.1029/2004PA001112.

Algeo, T.J. and Tribovillard, N. (2009) Environmental analysis of paleocenographic systems based on molybdenum-uranium covariation. *Chem. Geol*. **268**, 211-225.

Amini, M. Weis, D., Soon, M. and Francois, R. (2016) Molybdenum Isotope Fractionation in Saanich Inlet, British Columbia. *Goldschmidt Conference, Yokohama,***60**.

Andersen, M., Stirling, C., Zimmermann, B. and Halliday, A. (2010) Precise determination of the open ocean $^{234}U/^{238}U$ composition. *Geochem. Geophys. Geosyst.* **11**, doi.org/10.1029/2010GC003318.

Andersen, M.B., Vance, D., Keech, A.R., Rickli, J. and Hudson, G. (2013) Estimating U fluxes in a high-latitude, boreal post-glacial setting using U-series isotopes in soils and rivers. *Chem. Geol.* **354**, 22-32.

Andersen, M.B., Romaniello, S., Vance, D., Little, S.H., Herdman, R. and Lyons, T.W. (2014) A modern framework for the interpretation of $^{238}U/^{235}U$ in studies of anciend ocean redox. *Earth Planet. Sci. Lett.* **400**, 184-194.

Andersen, M.B., Elliott, T., Freymuth, H., Sims, K.W., Niu, Y. and Kelley, K.A. (2015) The terrestrial uranium isotope cycle. *Nature* **517**, 356-359.

Andersen, M.B., Vance, D., Morford, J.L., Bura-Nakić, E., Breitenbach, S.F.M. and Och, L . (2016) Closing in on the marine $^{238}/^{235}U$ budget. *Chem. Geol.* **420**, 11-22.

1 Andersen, M.B., Stirling, C.H. and Weyer, S. (2017) Uranium isotope fractionation. *Reviews*
2 *in Mineralogy & Geochemistry* **82**, 799-850.

3 Anderson, R.F. (1987) Redox behaviour of uranium in an anoxic marine basin. *Uranium* **3**, 145-
4 164.

5 Anderson, R.F., Fleischer, M.Q. and LeHurray, A.P. (1989a) Concentration, oxidation state,
6 and particulate flux of uranium in the Black Sea. *Geochim. Cosmochim. Acta* **53**, 2215-
7 2224.

8 Anderson, R.F., LeHuray, A.P., Fleisher, M.Q. and Muray, W. (1989b) Uranium deposition in
9 Saanich Inlet sediments, Vancouver Island. Geochim. Cosmochim. Acta **53**, 2202-2213.

10 Archer, C. and Vance, D. (2008) The isotopic signature of the global riverine molybdenum flux
11 and anoxia in the ancient oceans. *Nature Geoscience* **1**, 597-600.

12 Arnold, G.I., Anbar, A.D., Barling, J. and Lyons, T.W. (2004) Molybdenum isotope evidence
13 for widespread anoxia in mid-proterozoic oceans. *Science* **304**, 87-90.

14 Azrieli-Tal, I., Matthews, A., Bar-Matthews, M., Almogi-Labin, A., Vance, D., Archer, C. and
15 Teutsch, N. (2014) Evidence from molybdenum and iron isotopes and molybdenum-
16 uranium covariation for sulphidic bottom waters during Eastern Mediterranean sapropel
17 S1 formation. *Earth Planet. Sci. Lett.* **393**, 231-242.

18 Bargar, J.R., Williams, K.H., Campbell, K.M., Long, P.E., Stubbs, J.E., Suvorova, E.I.,
19 Lezama-Pacheco, J.S., Alessi, P.S., Stylo, M., Webb, S.M., Davis, J.A., Giammar, D.E.,
20 Blue, L.Y. and Bernier-Latmani, R. (2013) Uranium redox transformation pathways in
21 acetate-amended sediments. *Proc. Natl. Acad. Sci. U.S.A.* **110(12)**, 4506-4511.

22 Barling, J., Arnold, G.L. and Anbar, A.D. (2001) Natural mass-dependent variations in the
23 isotopic composition of molybdenum. *Earth Planet. Sci. Lett.* **193**, 447-457.

1 Barling, J. and Anbar, A.D. (2004) Molybdenum isotope fractionation during adsorption by
2 manganese oxides. *Earth Planet. Sci. Lett.* **217**, 315-329.

3 Barnes, C.E, and Cochran, J.K. (1990) Uranium removal in oceanic sediments and the oceanic-
4 U balance. *Earth Planet. Sci. Lett.* **97**, 94-101.

5 Basu, A., Stanford, R.A., Johnson, T.M ., Lundstrom, C.C . and Löfller, F.E. (2014) Uranium
6 isotopic fractionation factors during U(VI) reduction by bacterial isolates. *Geochim.*
7 *Cosmochim. Acta* **136**, 100-113.

8 Bender, M.L. (1990) The $\delta^{18}O$ of dissolved O_2 in seawater: a unique tracer of circulation and
9 respiration in the deep sea. *J. Geophys. Res., Oceans* **95**, 22242-22252.

10 Bigeleisen, J. (1996) Nuclear size and shape effects in chemical reactions. Isotope chemistry of heavy
11 elements. *J. Amer. Chem. Soc.* **118**, 3676-3680.

12 Bostick, B.C., Fendore, S. and Helz, G.R. (2003) Differential adsorption of molybdate and
13 tetrathiomolybdate on pyrite (FeS_2). *Environ. Sci. Technol.* **37**, 285-291.

14 Brennecka, G.A., Herrmann, A.D., Alego, T.J. and Anbar, A.D. (2011a) Rapid expansion of
15 oceanic anoxia immediately before the end-Permian mass extinction. *Proc. Natl. Acad.*
16 *Sci.* **108**, 17631-17634.

17 Brennecka, G.A., Wasylenki, L.E., Bargar, J.R., Weyer, S. and Anbar, A.D. (2011b) Uranium
18 isotope fractionation during adsorption to Mn-oxyhydroxides. *Environ. Sci. Technol.*
19 **45**,1370-1375.

20 Bura-Nakić, E., Helz, G.R., Ćosović, B. and Ciglenečki, I. (2009) Reduced sulfur species in a
21 stratified seawater lake (Rogoznica Lake, Croatia); seasonal variations and evidence for
22 organic carriers of reactive sulfur. *Geochim. Cosmochim. Acta* **73**, 3738–3751.

Cheng, H., Edwards, R.L., Sehe, C.C ., Polyak, V.J., Asmerom, Y., Woodhead, Y., Hellstrom, J., Wang, Y., Kong, X., Spötl, C., Wang, X. and Alexander Jr., C. (2013) Improvements in ^{230}Th dating, ^{230}Th and ^{234}U half-life values, and U-Th isotopic measurements by multi-collector inductively couples plasma mass spectrometry. *Earth Planet. Sci. Lett.* **371-372**, 82-91.

Ciglenečki, I., Janeković, I., Marguš, M., Bura-Nakić, E., Carić, M., Ljubešić, Z., Batistić, M., Hrustić, E., Dupčić, I. and Garić, R. (2015) Impacts of extreme weather events on higly eutrophic marine ecosystem (Rogoznica Lake, Adriatic coast). *Cont. Shelf Res.* 1**08**, 144-155.

Ciglenečki, I., Carić, M., Kršinić, F., Viličić, D. and Ćosović, B. (2005) The extintion by sulfide - turnover and recovery of a naturally eutrophic, meromictic seawater lake. *J. Mar. Sys*. **56**, 29-44.

Clark, S.K. and Johnson, T.M. (2008) Effective isotopic fractionation factors for solute removal by reactive sediments: a laboratory microcosm and slurry study. *Environ. Sci. Technol.* **42**, 7850-7855.

Collier, R.W. (1985) Molybdenum in the Northeast Pacific Ocean. *Limnol. Oceanogr.* **30**, 1351-1354.

Colodner, D., Edmond, J. and Boyle, E. (1995) Rhenium in the Black Sea: comparison with molybdenum and uranium. *Earth Planet. Sci. Lett.* **131**, 1-15.

Dahl, T.W., Anbar, A.D., Gordon, G.W., Rosing, M.T., Frei, R. and Canfield, D.E. (2010) The behavior of molybdenum and its isotopes across the chemocline and in the sediments of sulfidic Lake Cadagno, Switzerland. *Geochim. Cosmochim. Acta* **74**, 144-163.

Emerson, S.R. and Huested, S.S. (1991) Ocean anoxic and the concentration of molybdenum and vanadium in seawater. *Mar. Chem*. 3**4**, 177-196.

Erickson, B.E., and Helz, G.R. (2000) Molybdenum (VI) speciation in sulphidic waters: stabiity and lability of thiomolybdates. *Geochim. Cosmochim. Acta* **64**, 1149-1158.

Goldberg, T., Archer, C., Vance, D. and Poulton, S.W. (2009) Mo isotope fractionation during adsorption to Fe (oxyhydr)oxides. *Geochim. Cosmochim. Acta* **73**, 6502-6516.

Fujii, Y., Higuchi, N., Haruno, Y., Nomura, M. and Suzuki, T. (2006) Temperature dependence of isotope effects in uranium chemical exchange reactions. *J. Nucl. Sci. Technol.* **43**, 400–406.

Gordon, G.W., Lyons, T.W., Arnold, G.L., Roe, J., Sageman, B.B. and Anbar, A.D. (2009) When do black shales tell molybdenum isotope tales? *Geology* **37**, 535-538.

Helz, G.R., Miller, C.V., Charnock, J.M., Mosselmans, J.F.W., Pattrick, R.A.D., Garner, C.D. and Vaughan, D.J. (1996) Mehanism of molybdenum removal from the sea and its concentration in black shales: EXAFS evidence. *Geochim. Cosmochim. Acta* **60**, 3631-3642.

Helz, G.R., Bura-Nakić, E., Mikac, N. and Ciglenečki, I. (2011) New model for molybdenum behavior in euxinic waters. *Chem. Geol*. **284**, 323-332.

Herrmann, A.D., Kendall, B., Alego, T.J., Gordon, G.W., Wasylenki, L.E., and Anbar, A.D. (2012) Anomalous molybdenum isotope trends in Upper Pennsylvanian euxinic facies: Significance for use of ^{98}Mo as a global marine redox proxy. *Chem. Geol*. **324-325**, 87-98.

Hinojosa, J.L., Stirling, C.H., Reid, M.R., Moy, C.M. and Wilson, G.S. (2016) Trace metal cycling and ^{238}U/^{235}U in New Zealand's fjords: Implications for reconstructing global paleoredox conditions in organic-rich sediments. *Geochim. Cosmocim. Acta* **179**, 89-109.

Holmden, C., Amini, M. and Francois, R. (2015) Uranium isotope fractionation in Saanich Inlet: A modern analog study of a paleoredox tracer. *Geochim. Cosmochim. Acta* **153**, 202-215.

Kerl, C.F., Lohmayer, R., Bura-Nakić, E., Vance, D. and Planer-Friedrich, B. (2017) Experimental confirmation of isotope fractionation in thiomolybdates using ion chromatography and detection by multi-collector ICP-MS. *Anal. Chem.* **89**, 3123-3129.

Klinkhammer, G.P. and Palmer, M.R. (1991) Uranium in the oceans: where it goes and why. *Geochim. Cosmochim. Acta* **55**, 1799-1806.

Kowalski, et al. (2013): Pelagic molybdenum concentration anomalies and the impact of sediment resuspension on the molybdenum budget in two tidal systems of the North Sea. Geochim. Cosmochim. Acta, 119, 198-211. dx.doi.org/10.1016/j.gca.2013.05.046

Ku, T.L., Knauss, K.G. and Mathieu, G.G. (1977) Uranium in open ocean: concentration and isotopic composition. *Deep-Sea Res.* **24**, 1005-1017.McLennan, S.M. (2001) Relationships between the trace element composition of sedimentary rocks and upper continental crust. *Geochem.Geophys. Geosyst.* **2**, doi: 10.1029/2000GC000109.

Lovley, D.R., Phillips, E.J.P., Gorby, Y.A., Landa, E.R., 1991. Microbial Reduction of Uranium. Nature 350, 413-416McManus, et al. (2002): Oceanic molybdenum isotope fractionation: Diagenesis and hydrothermal ridge-flank alteration. Geochemistry, Geophysics, Geosystems, 3 (12), 1078,doi:10.1029/2002GC000356,2002.

McManus, J., Berelson, W.M., Klinkhammer, G.P., Hammond, D.E. and Holm, C. (2005) Authigenic uranium: relationship to oxygen penetration depth and organic carbon rain. *Geochim. Cosmochim. Acta* **69**, 95-108.

McManus, J., Berelson, W.M., Severmann, S., Poulson, R.I., Hammond, D.E., Klinkhammer, G.P. and Holm, C. (2006) Molybdenum and uranium geochemistry in continental margin sediments: paleoproxy potential. *Geochim. Cosmochim. Acta* **70**, 4643-4662.

Millero, F.J. (1986) The thermodynamic and kinetics of the hydroge sulfide system in natural waters. *Mar. Chem.* **18**, 121-147.

Montoya-Pino, C,, Weyer, S., Anbar, A.D.,Pross, J., Oschmann, W., van de Schootbruuge, B. and Arz, H.W (2010) Global enhancment of ocean anoxia during Anoxic Oceanic Event 2: A quantitative approach using U isotopes. *Geology* **38**, 315-318.

Morford, J.L. and Emerson, S. (1999) The geochemistry of redox sensitive trace metals in sediments. *Geochim. Cosmochim. Acta* **63**, 1735-1750.

Nägler, T.F., Neubert, N., Böttcher, M.E., Dellwig, O. and Schnetger,B. (2011) Molybdenum isotope fractionation in pelagic euxinia: Evidence from the modern Black and Baltic Seas. *Chem. Geol*. **289**, 1-11.

Nägler, T.F., Anbar, A.D., Archer, C., Goldberg, T., Gordon, G.W., Greber, N.D., Siebert, C., Sohrin, Y. and Vance, D. (2014) Proposal for an international molybdenum isotope measurement standard and data representation. *Geostand. Geoanal. Res.* **38**, 149-151.

Nakagawa, Y., Takano, S., Firdaus, M.L., Norisuye, K., Hirata, T., Vance, D. and Sohrin, Y. (2012) The molybdenum isotopic composition of the modern ocean. *Geochem. J.* **46**, 131-141.

Noordmann, J., Weyer, S., Montoya-Pino, C., Dellwig, O., Neubert, N. and Eckert, S. (2015) Uranium and molybdenum isotope systematics in modern euxinic basins: Case studies from the central Baltic Sea and the Kyllaren fjord (Norway). *Chem. Geol*. **396**, 182-195.

Poulson, R.L., Siebert, C., McManus, J., Severmann, S. and Berelson, W.M. (2006) Authigenic molybdenum isotopes signatures in marine sediments. *Geology*, **34**, 617-620.

Poulson Brucker, R.L., McManus, J., Severmann, S. and Berelson, W.M. (2009) Molybdenum behavior during early diagenesis: insights from Mo isotopes. *Geochem. Geophy. Geosyst.* **10**, doi:10.1029/2008GC002180.

Prospero, J. M. (1996). Saharan dust transport over the North Atlantic Ocean and Mediterranean: an overview. In *The impact of desert dust across the Mediterranean* (eds. Guerzoni, S. and Chester R.). Netherlands, Springer, pp. 133-151.

Richter, S., Alonso-Munoz, A., Eykens, R., Jacobsson, U., Kuehn, H., Verbruggen, A., Aregbe, Y., Wellum, R. and Keegan, E. (2008). The isotopic composition of natural uranium samples-Measurements using the new n(^{233}U)/n(^{236}U) dobule spike IRMM-3636. *Int. J. Mass Spectrom.* **269**, 146-148.

Rolison, J.M., Stirling, C.H., Middag, R. and Rijkenberg, M. J.A. (2017) Uranium stable isotope fractionation in the Black Sea: modern calibration of the ^{238}U/^{235}U paleo-redox proxy. *Geochim. Cosmochim. Acta* **203**, 69-88.

Russell, A.D. and Morford, J.L. (2001) The behaviour of redox-sensitive metals across a laminated - massive-laminated transition in Saanich Inlet, British Columbia. *Marine Geology.* **174**, 341-354.

Scheiderich, K., Zerkle, A.L., Helz, G.R., Farquhar, J. and Walker, R.J. (2010) Molybdenum isotope, multiple sulfur isotope, and redox sensitive elementa behavior in early Pleistocene Mediterranean Sapropels. *Chem. Geo*l. **279**, 134-144.

Scott, C., Lyons, T.W., Bekker, A., Shen, Y., Poulton, S.W., Chu, X. and Anbar, A.D. (2008) Tracing the stepwise oxygenation of the Proterozoic ocean. *Nature* **452**, 456-459.

Siebert, C., Nägler, T.F., von Blanckenburg, F. and Kramers, J.D. (2003) Molybdenum isotope records as a potential new proxy for paleocenography. *Earth Planet. Sci. Lett.* **211**, 159-171.

Siebert, C., McManus, J., Bice, A., Poulson, R. and Berelson, W.M. (2006) Molybdenum isotope signatures in continental margin marine sediments. *Earth Planet. Sci. Lett.* **241**, 723-733.

Stirling, C.H., Andersen, M.B., Potter, E.K. and Halliday, A.N. (2007) Low temperature isotopic fractionation of uranium. *Earth Planet. Sci. Lett.* **264**, 208-225.

Stirling, C.H., Andersen, M.B., Warthmann, R. and Halliday, A.N. (2015) Isotope fractionation of ^{238}U and ^{235}U during biologically-mediated uraium reduction. *Geochim. Cosmochim. Acta* **163**, 200-218.

Stylo, M., Neubert, N., Wang, Y., Monga, N., Romaniello, S.J. and Weyer, S. (2015) Uranium isotopes fingerprint biotic reduction. *Proc. Natl. Acad. Sci.* **112**, 5619-5624.

Taylor, R.N. and McLennan, S. (1985) *The Continental Crust: Its Composition and Evolution.* Blackwell, Boston.

Tissot, F.L.H. and Dauphas, N. (2015) Uranium isotopic compositions of the crust and ocean: age corrections, U budget and global extent of modern anoxia. *Geochim. Cosmochim. Acta* **167**,113-143.

Tossell, J.A. (2005) Calculating the partitioning of the isotopes of Mo between oxidic and sulfidic species in aqueous solution. *Geochim. Cosmochim. Acta* **69**, 2981-2993.

Tribovillard, N., Alego, T., Lyons, T.W. and Riboulleau, A. (2006) Trace metals as paleoredox and paleoproductivity proxies: an update. *Chem. Geol.* **232**, 12-32.

Tribovillard, N., Alego, T.J., Baudin, F. and Riboulleau, A. (2012) Analysis of marine environmental conditions based on molybdenum - uranium covariation - Applications to Mesozoic paleocenography. *Chem. Geol*. **324-325**, 46-58.

Vogelin, A.R., Nägler, T.F., Samankassou, E. and Villa, I.M. (2009) Molybdenum isotopic composition of modern and Carboniferous carbonates. *Chem. Geol*. **265**, 488-498.

Vogelin, R.A., Nägler, T.F., Beukes, N.J. and Lacassie, J.P. (2010) Molybdenum isotopes in late Archean carbonate rocks: Implications for early Earth oxygenation. *Precambrian Res.* **182**, 70-82.

Vogelin, A.R., Pettke, T., Greber, N.D., von Niderhäusen, B. and Nägler, T. (2014) Magma differentiation fractionates Mo isotopes ratios: evidence from the Kos Plateau Tuff (Aegean Arc). *Lithos* **190-191**, 440-448.

Vorlicek, T.P., and Helz, G.R. (2002) Catalysis by mineral surfaces: implications for Mo geochemistry in anoxic environments. *Geochim. Cosmochim. Acta* **66**, 3679-3692.

Wang, X., Johnson, T.M. and Lundstrom, C.C., 2015. Isotope fractionation during oxidation of tetravalent uranium by dissolved oxygen. *Geochim. Cosmochim. Acta* **150**, 160–170.

Westermann, S., Vance, D., Cameron, V., Archer, C. and Robinson, S.A. (2014) Heterogeneous oxidation states in the Atlantic and Tethys oceans during Oceanic Anoxic Event 2. *Earth Planet. Sci. Lett.* **404**, 178-189.

Weyer, S., Anbar, A.D., Gerdes, A., Gordon, G.W., Alego, T.J. and Boyle, E.A. (2008) Natural fractionation of $^{238}U/^{235}U$. *Geochim. Cosmochim. Acta* **72**, 345-359.

Zheng, Y., Anderson, R.F., van Geen, A., Fleischer, M.Q., 2002. Preservation of particulate non-lithogenic uranium in marine sediments. Geochimica et Cosmochimica Acta 66, 3085-309

Figure captions

Figure 1: Depth–time sections for salinity, oxygen, sulfide, and particulate Fe and Mn concentrations in Lake Rogoznica during 2013 (February, April, July and October) and 2015 (April and July).

Figure 2: Depth profiles of dissolved (salinity normalised) and particulate Mo and U concentrations, dissolved and particulate δ^{98}Mo and δ^{238}U. The very high Mo concentration at the surface (0 m) in April and July 2013, as well as the low δ^{238}U in July 2013 (7.5 m), are given as numerical values.

Figure 3: Authigenic sedimentary and pore water Mo and U concentrations, as well as δ^{98}Mo and δ^{238}U, in the sediment core recovered from the anoxic portion of Lake Rogoznica, plotted versus depth beneath the sediment water interface. The dashed lines on all four plots show the isotopic composition of the open ocean for Mo and U.

Figure 4: A: Mo isotopic composition plotted against reciprocal Mo concentration for all samples with $O_2 > 5 mg\ l^{-1}$. Most data fall along a flat trajectory close to oceanic Mo isotope ratios at variable Mo concentrations (horizontal grey arrow). Some data for April and July 2013, however, show higher Mo concentrations and lower δ^{98}Mo, lying along a trajectory that requires an extra source of Mo with δ^{98}Mo around +0.4 to +0.5‰. B: $\delta^{98}Mo_{diss\text{-}part}$ for all dissolved-particulate pairs, including sediment-pore water, for samples where sulfide is detectable. The water column data appear to become asymptotic to a value around +0.3‰ at very high dissolved sulfide concentrations. Though pore water data are more scattered, no $\delta^{98}Mo_{diss\text{-}part}$ is below this value.

Figure 5: A: Salinity-normalised [U] data from the February 2013 campaign (red diamonds); the modelled thick black line on the diagram is for a virtually stagnant lake (no advection) in which U diffuses downwards into the sediment. The relative importance of advection versus

diffusion is represented by the value of ω/D, which is ~0.007 for the modelled evolution. For comparison, the thin dashed line shows a profile dominated by advection, with a ω/D = 0.7, two orders of magnitude greater. B: All data from the four intermediate sampling campaigns. C: Data from the July 2015 campaign (purple circles). The water column is separated into two rather isolated layers above and below the chemocline. The black curve shows the impact of transport within each layer that is completely dominated by advection over diffusion (ω/D = 2±0.3) - both reservoirs are well mixed for [U] with much slower communication across the chemocline.

Figure 6: Salinity-normalised [U] vs. $\delta^{238}U$ for Lake Rogoznica. A: Data from the February 2013 campaign (red diamonds), which, as for [U] (Fig 5), most closely follow the expected trajectory for diffusion-driven U removal from a stagnant water column. The red dotted line is a regression of the data (based on 1/[U] vs $\delta^{238}U$). The curved solid black line shows the approximate trajectory expected for the waters, with diffusion-driven U removal with a +0.6‰ difference in the removal rate constants for ^{238}U and ^{235}U, and a starting composition similar to water sample with the highest [U] (see supplementary text for details). The dashed line shows the trajectory for removal within the water column via a Rayleigh process with a 1.2‰ fractionation in $^{238}U/^{235}U$, starting from the same water sample as the diffusion model. B: All data from the four intermediate sampling campaigns. C: Data for July 2015 (purple circles) which, again like the [U] data (Fig 5), show strong asymmetry. This profile is characterised by an upper oxic layer that is near homogeneous in [U] and $\delta^{238}U$ because of isolation from the sediment by a strong chemocline, and a lower anoxic layer. The [U]-$\delta^{238}U$ systematics in the lower anoxic layer (1/[U] vs $\delta^{238}U$ regression; dotted line) follow the model trajectory for diffusion-driven U removal from a stagnant water column (solid line), with the deepest oxic sample, nearest the chemocline, used as the upper boundary for both the regression line and diffusion modelling.

Figure 7: Relationship between $\delta^{238}U_{auth}$ and (i) the percentage of dissolved U removal in deep anoxic vs surface water (bottom axis, open symbols, blue regression line) and (ii) total dissolved sulfide (ΣS^{2-}) in the anoxic part of the water column (closed symbols, red regression line). Sulfide concentrations in Supplementary Table 2. See Table 1 for citations to data. The slope of the U removal vs. $\delta^{238}U_{auth}$ best fit regression line is close to that expected for diffusive removal U flux with an effective $^{238}U/^{235}U$ fractionation ~+0.6 (see supplementary text).

Figure 8: A: U vs Mo enrichment factors and, B: authigenic $\delta^{98}Mo$ vs. $\delta^{238}U$, for Lake Rogoznica sediments (individual sediment horizons, open circles; average, filled circle) compared to other euxinic basins. Key to colours for both panels as indicated in Panel B. Data sources: Kyllaren Fjord (Noordmann et al., 2015), Black Sea (Station 9 data in Arnold et al., 2004; Andersen et al., 2014), Cariaco Basin (Arnold et al., 2004; Andersen et al., 2014), Saanich Inlet (Russell and Morford, 2001; Holmden et al., 2015; Amini et al., 2016). In A the seawater Mo/U is plotted as the solid line, with deviations from the seawater ratio shown as dashed lines as indicated. In B schematic solid arrows show how sediment deposited beneath euxinic waters would vary in different euxinic basins for high versus low rates of Mo removal relative to U, assuming a constant fractionation factor for uranium isotopes. These scenarios would require Mo fractionation during initial non-quantitative removal to be substantial, but more subtle during the subsequent more quantitative removal, consistent with theoretical, experimental and observational constraints (e.g. Helz et al., 1996; Tossel, 2005; Nägler et al., 2011; Kerl et al., 2017).

Table 1: $[\Sigma S^{-II}]$, $[U]_{diss}$ and $\delta^{238}U$ of dissolved ($\delta^{238}U_{diss}$) and authigenic sedimentary ($\delta^{238}U_{auth}$) uranium in the anoxic water columns and sediments of different modern anoxic basins.

Euxinic basin	Salinity norm. $[U]_{diss}$ nmol l^{-1} **	$\delta^{238}U_{auth}$ in sediments	$\delta^{238}U_{diss}$ deep waters	$[\Sigma S^{-II}]$ µmol l^{-1} deep waters	Source
Lake Rogoznica*	2.8/***	-0.30	-0.94	1214	This work
Kyllaren Fjord	7.5/12.9	-0.22	-0.71	4316	Noordmann et al. (2015)
Black Sea	9.3/17.3	-0.03	-0.68	262	Rolison et al. (2016)
Cariaco Trench	12.0/14.5	+0.03	-	40	Anderson (1987) Emerson and Huested (1991) Andersen et al. (2014)
Saanich Inlet	14.7/15.4	+0.17	-0.48	30	Emerson and Huested (1991) Holmden et al. (2015)

*average values for $[U]_{diss.}$, $\delta^{238}U_{auth}$, $\delta^{238}U_{diss.}$ and ΣS^{-II} in the deepest anoxic Lake Rogoznica samples from all 6 sampling events.

*Salinity normalised (35) U concentrations for deep waters/surface waters. This ratio is used for the U water column removal fraction in Figure 7.

***A [U] as the open ocean was used for the surface waters (13.4 $nmol^{-1}$) in this setting.

Figure 1

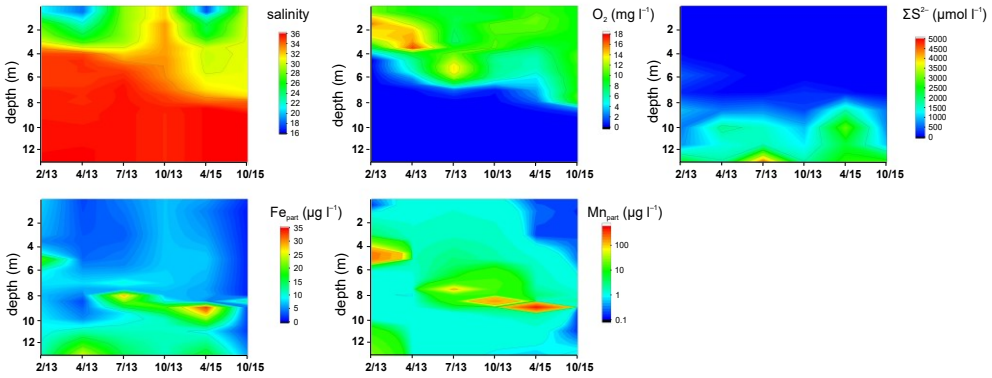
salinity
O2 (mg l-1)
ΣS2- (µmol l-1)
Fepart (µg l-1)
Mnpart (µg l-1)
depth (m)
2/13
4/13
7/13
10/13
4/15
10/15

Figure 2

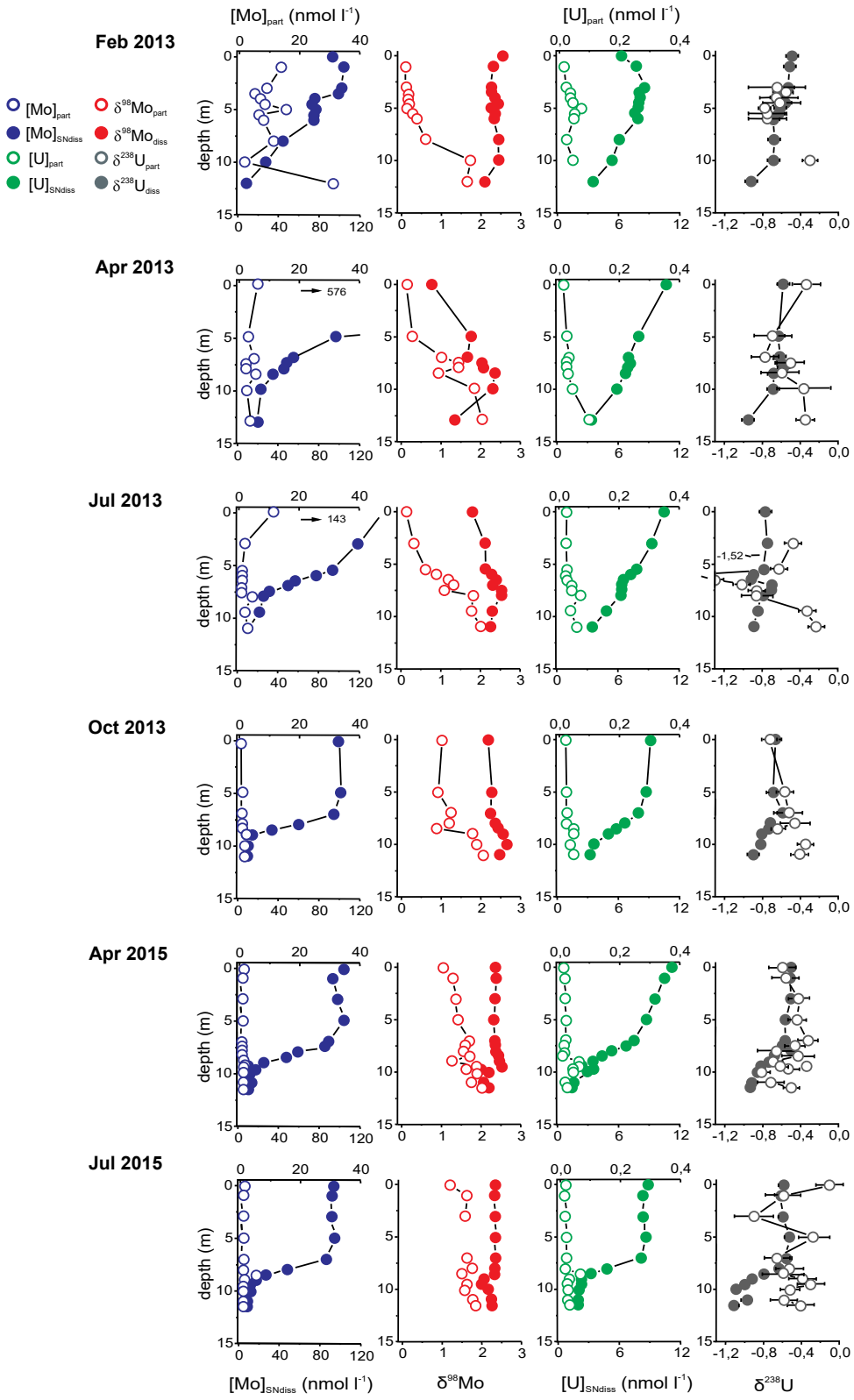
[Mo]part (nmol l-1)
[U]part (nmol l-1)
Feb 2013
Apr 2013
Jul 2013
Oct 2013
Apr 2015
Jul 2015
[Mo]part
[Mo]SNdiss
[U]part
[U]SNdiss
δ98Mopart
δ98Modiss
δ238Upart
δ238Udiss
depth (m)
576
143
-1,52
[Mo]SNdiss (nmol l-1)
δ98Mo
[U]SNdiss (nmol l-1)
δ238U

Figure 3

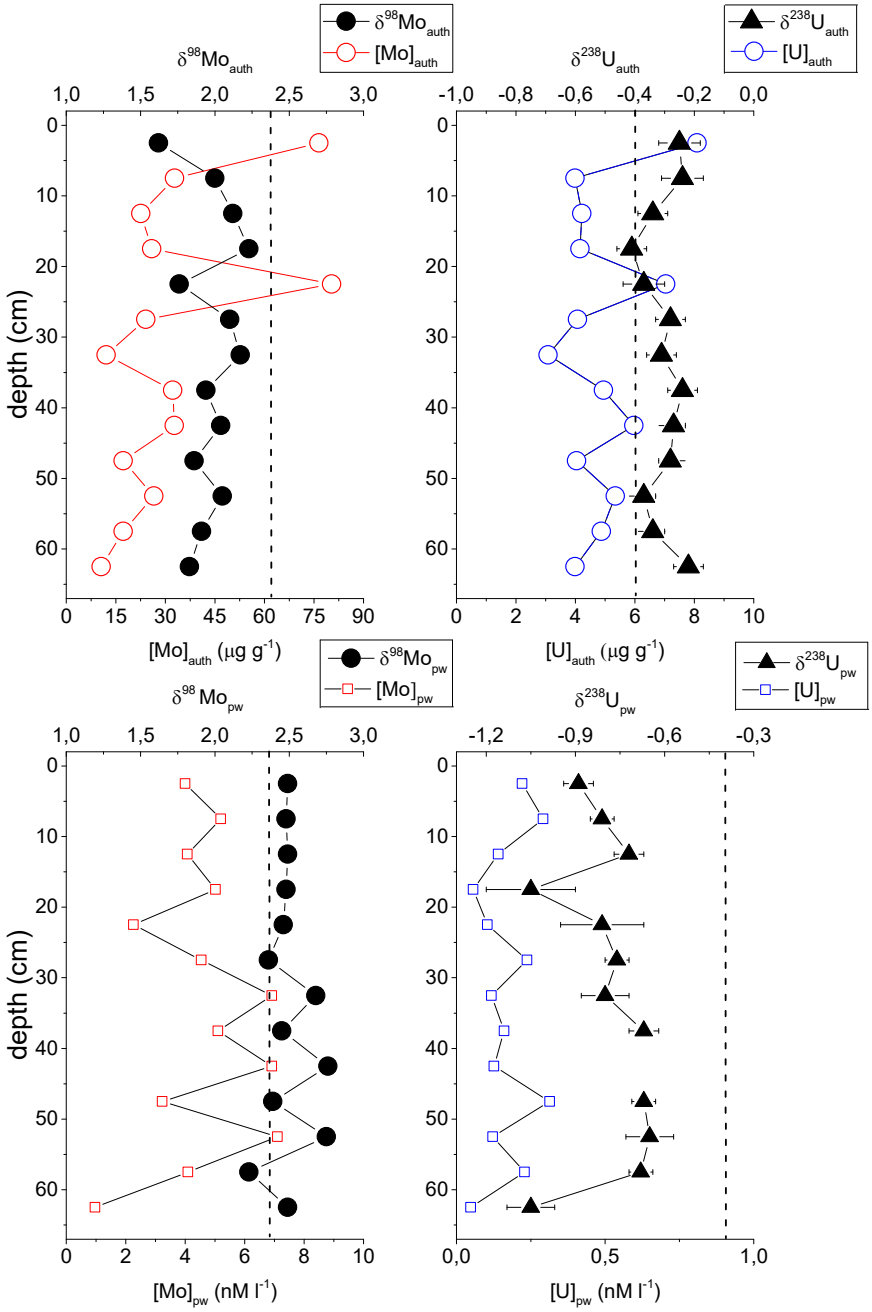
δ98Moauth
[Mo]auth
δ98Mo
δ238Uauth
[U]auth
depth (cm)
[Mo]auth (µg g-1)
[U]auth (µg g-1)
δ98Mopw
[Mo]pw
δ98 Mopw
δ238Upw
[U]pw
[Mo]pw (nM l-1)
[U]pw (nM l-1)

Figure 4

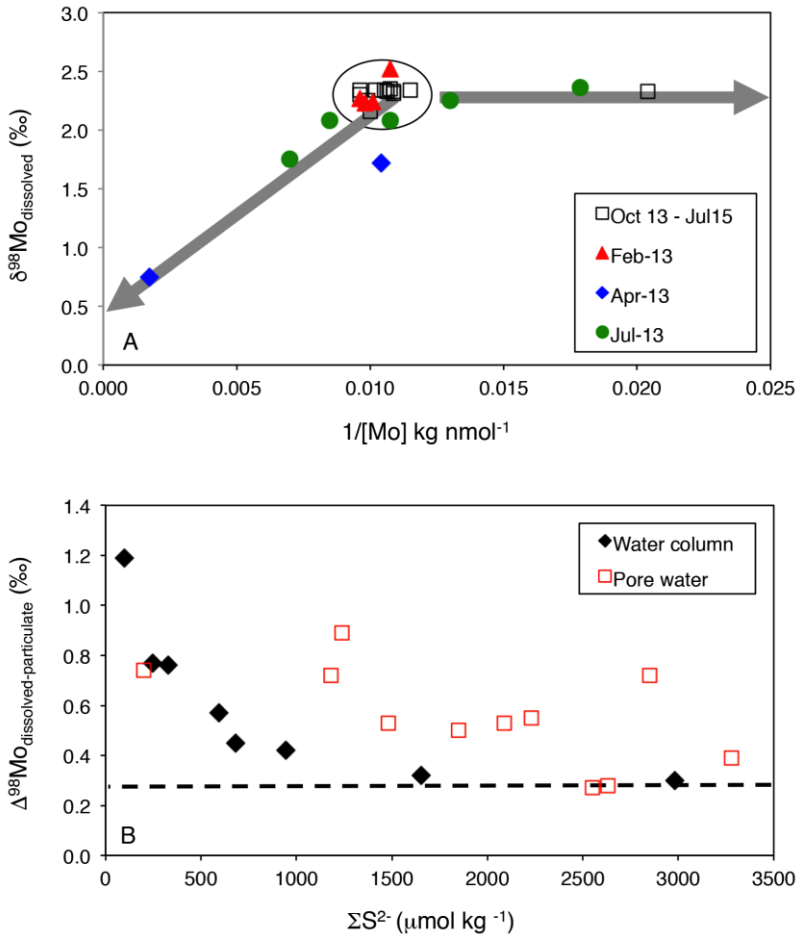
3.0
2.5
2.0
1.5
1.0
0.5
0.0
δ98Modissolved (‰)
A
Oct 13 - Jul15
Feb-13
Apr-13
Jul-13
0.000
0.005
0.010
0.015
0.020
0.025
1/[Mo] kg nmol-1
1.4
1.2
1.0
0.8
0.6
0.4
0.2
0.0
Δ98Modissolved-particulate (‰)
B
Water column
Pore water
0
500
1000
1500
2000
2500
3000
3500
ΣS2- (μmol kg -1)

Figure 5

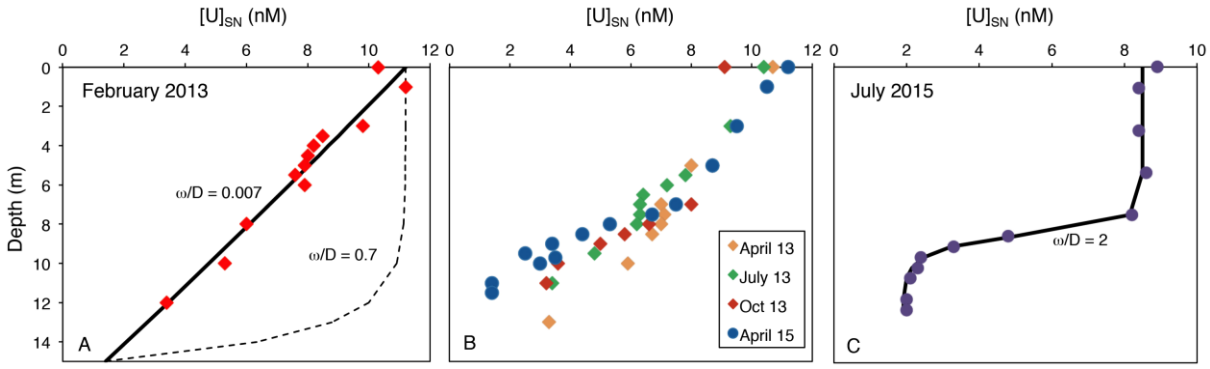
[U]SN (nM)
Depth (m)
February 2013
ω/D = 0.007
ω/D = 0.7
A
B
April 13
July 13
Oct 13
April 15
July 2015
ω/D = 2
C

Figure 6

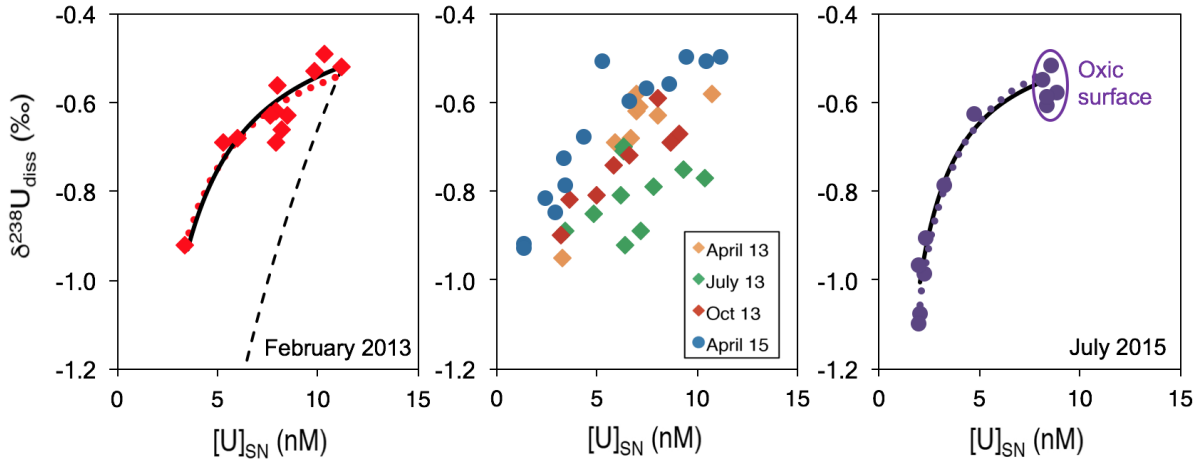
-0.4
-0.6
-0.8
-1.0
-1.2
δ238Udiss (‰)
0
5
10
15
[U]SN (nM)
February 2013
April 13
July 13
Oct 13
April 15
Oxic
surface
July 2015

Figure 7

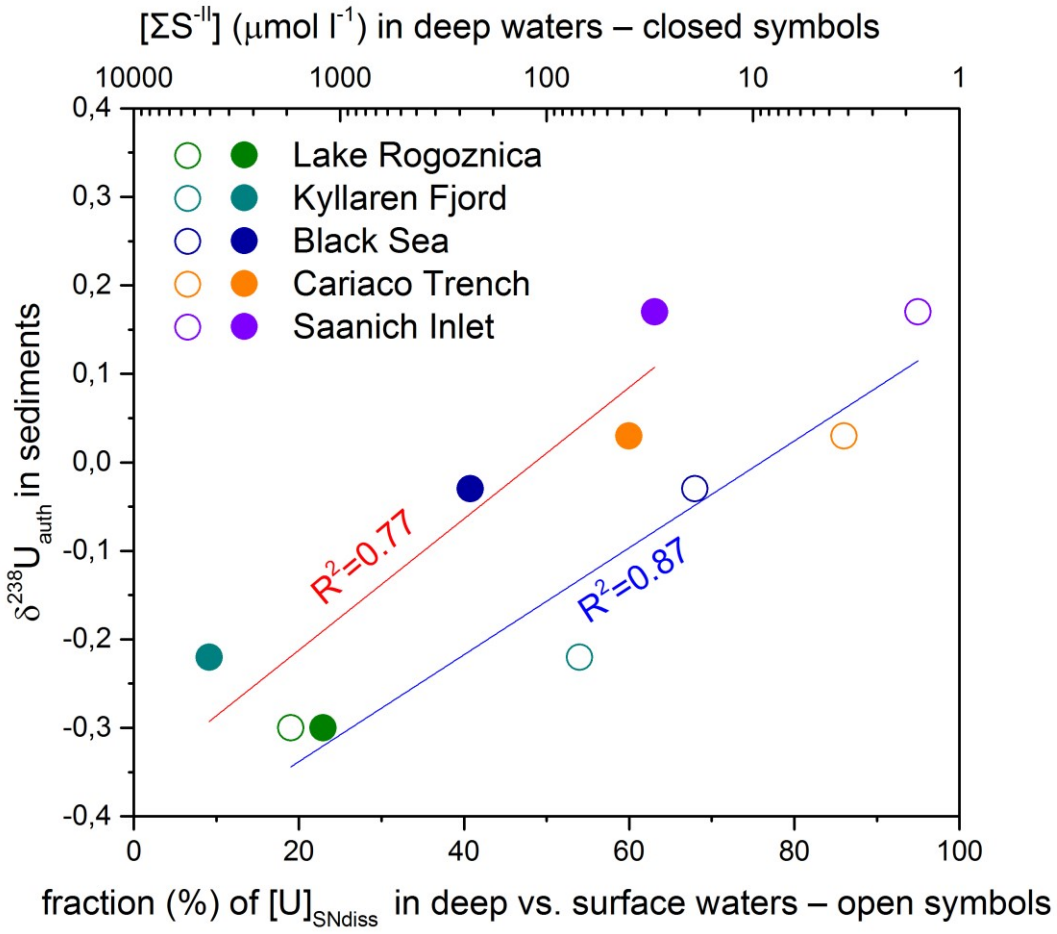
[ΣS-II] (μmol l-1) in deep waters – closed symbols
10000
1000
100
10
1
0,4
0,3
0,2
0,1
0,0
-0,1
-0,2
-0,3
-0,4
Lake Rogoznica
Kyllaren Fjord
Black Sea
Cariaco Trench
Saanich Inlet
R2=0.77
R2=0.87
δ238Uauth in sediments
0
20
40
60
80
100
fraction (%) of [U]SNdiss in deep vs. surface waters – open symbols

Figure 8

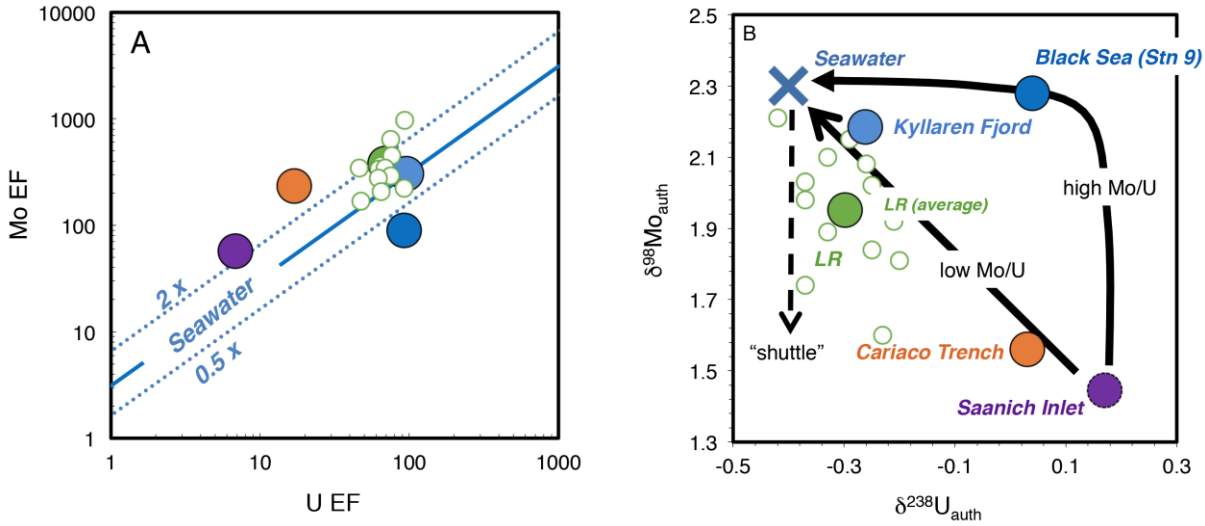
A
Mo EF
U EF
10000
1000
100
10
1
1
10
100
1000
2 x
Seawater
0.5 x
B
Seawater
Black Sea (Stn 9)
Kyllaren Fjord
high Mo/U
LR (average)
LR
low Mo/U
"shuttle"
Cariaco Trench
Saanich Inlet
δ98Moauth
δ238Uauth
2.5
2.3
2.1
1.9
1.7
1.5
1.3
-0.5
-0.3
-0.1
0.1
0.3